ANTIOXIDANTS & REDOX SIGNALING
Volume 21, Number 15, 2014

DOI: 10.1089/ars.2013.5565

Discoveries

ORIGINAL RESEARCH COMMUNICATION

Aldosterone Activates Transcription Factor Nrf2 in Kidney Cells Both *In Vitro* and *In Vivo*

Nina Queisser,[1] Patricia I. Oteiza,[2] Samuel Link,[1] Valentin Hey,[1] Helga Stopper,[1] and Nicole Schupp[1]

Abstract

Aims: An increased kidney cancer risk was found in hypertensive patients, who frequently exhibit hyperaldosteronism, known to contribute to kidney injury, with oxidative stress playing an important role. The capacity of kidney cells to up-regulate transcription factor nuclear factor-erythroid-2-related factor 2 (Nrf2), a key regulator of the cellular antioxidative defense, as a prevention of aldosterone-induced oxidative damage was investigated both *in vitro* and *in vivo*. ***Results:*** Aldosterone activated Nrf2 and increased the expression of enzymes involved in glutathione (GSH) synthesis and detoxification. This activation depended on the mineralocorticoid receptor (MR) and oxidative stress. *In vitro*, Nrf2 activation, GSH amounts, and target gene levels decreased after 24 h, while oxidant levels remained high. Nrf2 activation could not protect cells against oxidative DNA damage, as aldosterone-induced double-strand breaks and 7,8-dihydro-8-oxo-guanine (8-oxodG) lesions steadily rose. The Nrf2 activator sulforaphane enhanced the Nrf2 response both *in vitro* and *in vivo*, thereby preventing aldosterone-induced DNA damage. *In vivo*, Nrf2 activation further had beneficial effects on the aldosterone-caused blood pressure increase and loss of kidney function. ***Innovation:*** This is the first study showing the activation of Nrf2 by aldosterone. Moreover, the results identify sulforaphane as a substance that is capable of preventing aldosterone-induced damage both *in vivo* and *in vitro*. ***Conclusion:*** Aldosterone-induced Nrf2 adaptive response cannot neutralize oxidative actions of chronically increased aldosterone, which, therefore could be causally involved in the increased cancer incidence of hypertensive individuals. Enhancing the cellular antioxidative defense with sulforaphane might exhibit beneficial effects. *Antioxid. Redox Signal*. 21, 2126–2142.

Introduction

OXIDATIVE AND NITRATIVE STRESS act as predisposing factors to multistage carcinogenesis. Oxidative stress can either directly modify DNA and cause genetic alterations or influence epigenetic mechanisms, that is, by modulating cellular signal transduction pathways (17). In response to oxidative and nitrative stress, cells trigger signaling cascades, such as transcription factor nuclear factor-erythroid-2-related factor 2 (Nrf2), that up-regulate key defensive responses.

Nrf2 is essential for the coordinated induction of genes encoding many stress-responsive or cytoprotective enzymes and related proteins. Besides its role in regulating carcinogen detoxification and cellular antioxidant defense, Nrf2 also has anti-inflammatory functions (56). On oxidative/nitrative stress, Nrf2 is released from its repressor Kelch-like ECH-associated protein 1 (Keap1), translocates into the nucleus,

Innovation

This is the first study reporting that aldosterone, besides exhibiting adverse effects on the kidney and cardiovascular system when pathologically increased, is capable of activating a major cellular defense mechanism, transcription factor nuclear factor-erythroid-2-related factor 2 (Nrf2) and its activation pathway. This activation, nevertheless, is not sufficient to protect cells or animals from aldosterone-induced oxidative stress and DNA damage. However, further novel findings show that induction of the Nrf2 response with the isothiocyanate sulforaphane normalizes aldosterone-mediated hypertension, improves kidney function in rats, and, importantly, prevents oxidative DNA damage both *in vitro* and *in vivo*, which could probably reduce end-organ damage in hypertension.

[1]Department of Toxicology, University of Würzburg, Würzburg, Bavaria, Germany.
[2]Department of Nutrition and Department of Environmental Toxicology, University of California, Davis, Davis, California.

forms heterodimers with small Maf proteins, and binds to antioxidant response element (ARE) sequences or electrophile response element sequences present in the promotor/enhancer regions of genes encoding for antioxidant and detoxifying enzymes such as thioredoxin (*Txn1*), superoxide dismutase (*Sod1*), glutathione peroxidase (*Gpx*), or heme oxygenase-1 (*Hmox1*) (28, 55, 56). The Nrf2-mediated antioxidant response is one of the major cellular defense mechanisms that preserve cell function under toxic insults (32).

The mineralocorticoid aldosterone plays a major role in the maintenance of the electrolyte and fluid balance and subsequent blood pressure homeostasis. This is mediated by genomic actions *via* the mineralocorticoid receptor (MR). However, aldosterone also exerts rapid, nongenomic effects, among them being the production of ROS *via* NADPH oxidase (52). We recently found aldosterone to be genotoxic and to produce oxidative stress at very low concentrations in renal tubule cells (43, 49) and in rat kidneys (41). Aldosterone levels are increased in a subgroup of hypertensive patients with prevalence of 8%–13% (13, 47) and in patients with resistant hypertension, with a prevalence of 20% (5). The plasma concentration of aldosterone in these patients ranges from 0.5 to 6.3 n*M*, with patients suffering from congestive heart failure reaching 8 n*M* (47, 58), which is approximately 20 times higher than in healthy individuals (58). Epidemiological studies investigating a possible connection between hypertension and cancer found higher cancer mortality rates in hypertensive patients, and, in particular, an increased risk to develop renal cancer (12, 20). We postulate that the genotoxicity of increasing concentrations of aldosterone contributes to the hypertension-associated increased cancer risk.

This article investigated both *in vivo* and *in vitro* the capacity of renal cells to up-regulate Nrf2-mediated protective responses when exposed to high aldosterone levels. Furthermore, sulforaphane, a natural Nrf2 inducer, was tested to additionally enhance the Nrf2 response and to protect against aldosterone-induced DNA damage both *in vitro* and *in vivo*.

Results

Aldosterone activates Nrf2 in vivo *and* in vitro

In vivo study. Aldosterone activates Nrf2 and leads to the expression of Nrf2-regulated genes that are dependent on the MR and oxidative stress *in vivo.*

The *in vivo* activation of Nrf2 in rat kidneys as a consequence of hyperaldosteronism was investigated in rats treated with aldosterone, aldosterone/spironolactone, and aldosterone/tempol. Immunohistological staining showed that kidneys from aldosterone-treated rats had significantly higher levels of Nrf2-positive nuclei in the cortex and medulla (Fig. 1A, B and Supplementary Fig. S1; Supplementary Data are available online at www.liebertpub.com/ars), indicating the activation of transcription factor Nrf2 as a consequence of hyperaldosteronism. Representative pictures of the kidney are found in Supplementary Figure S1. Simultaneous treatment with aldosterone and the MR receptor blocker

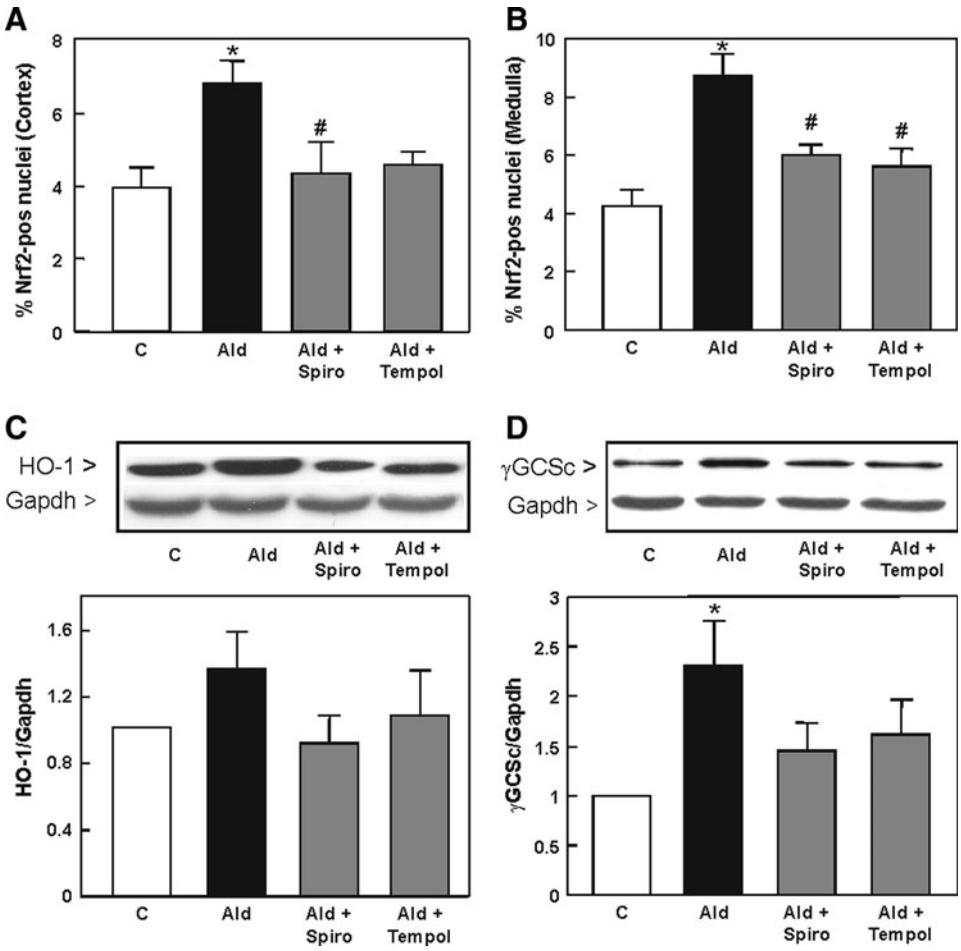

FIG. 1. Aldosterone induces Nrf2 activation and expression of Nrf2-regulated genes *in vivo* dependent on the MR and oxidative stress. Evaluation of immunohistochemical staining on paraffin-embedded kidney cortex and medulla sections for Nrf2 activation. The ratio of positive/negative nuclei was quantified by Cell Profiler within eight visual fields of **(A)** cortex and **(B)** medulla of the kidney. Expression of HO-1 (32 kDa) and γGCSc (73 kDa) in the rat kidney was evaluated by Western blot **(C, D)**. Representative images and the quantification of the HO-1 and γGCSc bands are shown. **(A–D)** Shown are mean values ± SEM, $^{*}p \le 0.05$ *versus* the control group, $^{\#}p \le 0.05$ *versus* the aldosterone-treated group, tested by ANOVA with subsequent *post-hoc* comparisons by Scheffé. HO-1, heme oxygenase-1; MR, mineralocorticoid receptor; Nrf2, nuclear factor-erythroid-2-related factor 2; γGCSc, γ-glutamylcysteine synthetase catalytic subunit.

spironolactone significantly reduced the occurrence of Nrf2-positive nuclei in rat kidneys. Treatment with aldosterone and the antioxidant tempol showed a significant reduction of Nrf2 nuclear abundance compared with the Ald group.

Since Nrf2 modulates the expression of genes involved in the protection against oxidative stress and detoxification, the expression of HO-1 and the GCL catalytic subunit γGCSc was measured by Western blot in rat kidneys. HO-1 was up-regulated in aldosterone-treated rat kidneys compared to the control, and lower in rats simultaneously treated with spironolactone and tempol (Fig. 1C). Protein levels of γGCSc were significantly higher in aldosterone-treated rat kidneys compared to the control. Neither spironolactone nor tempol had a significant impact on the up-regulation of both proteins (Fig. 1D).

In vitro experiments

Aldosterone induces the activation of Nrf2 in a pig kidney cell line. To confirm the results observed *in vivo*, the activation of Nrf2 by aldosterone was investigated in the pig kidney cell line LLC-PK1, which has characteristics of proximal tubule cells (33). Nrf2-DNA binding was measured in nuclear fractions by electrophoretic mobility shift assay (EMSA). The activation of Nrf2 in LLC-PK1 cells was dependent on the aldosterone concentration (5–100 n*M*). A slight increase in Nrf2-DNA binding was already observed at 10 n*M* aldosterone, although significance was reached after 0.5 h incubation with 50 and 100 n*M* of aldosterone (Fig. 2A). Subsequent EMSA experiments were conducted with 100 n*M* aldosterone to ensure a sufficiently high response; all other experiments were additionally carried out with 10 n*M* aldosterone.

The incubation of LLC-PK1 cells with 100 n*M* aldosterone caused an increase in nuclear Nrf2-binding, which reached maxima after 0.5 and 4 h incubation (Fig. 2B). The specificity of the Nrf2-DNA complex in the EMSA assay was assessed by competition with a 100-fold molar excess of unlabeled oligonucleotide (cold) containing the consensus sequence for either Nrf2 or SP-1. Nrf2 activation was further observed on measuring the presence of Nrf2 by Western blot. Nrf2 activation was significantly increased after 1, 2, and 4 h of treatment with 10 n*M* aldosterone (Fig. 2C) and after 2 and 4 h of treatment with 100 n*M* aldosterone (Fig. 2D). After 24 h, Nrf2 levels were reduced again.

Aldosterone-induced activation of Nrf2 leads to an increased expression of Nrf2-regulated genes. The expression of TRX, SOD, HO-1, and γGCSc was evaluated by measuring protein levels by Western blot. The expression of TRX was significantly increased after 1 h until 24 h with 10 n*M* aldosterone (Fig. 3A) and after 2, 4, and 24 h with 100 n*M* aldosterone (Fig. 3B). SOD levels were significantly up-regulated after 1, 2, and 4 h with 10 and 100 n*M* aldosterone (Fig. 3C, D). HO-1 levels were significantly increased after 4 h incubation with 10 n*M* aldosterone (Fig. 3E) and after 2 h incubation with 100 n*M* aldosterone (Fig. 3F). The expression of γGCSc was significantly increased after 0.5 h incubation with 10 and 100 n*M* of aldosterone (Fig. 4A, B). Nevertheless, after 24 h, the expression of both HO-1 and γGCSc returned to basal levels.

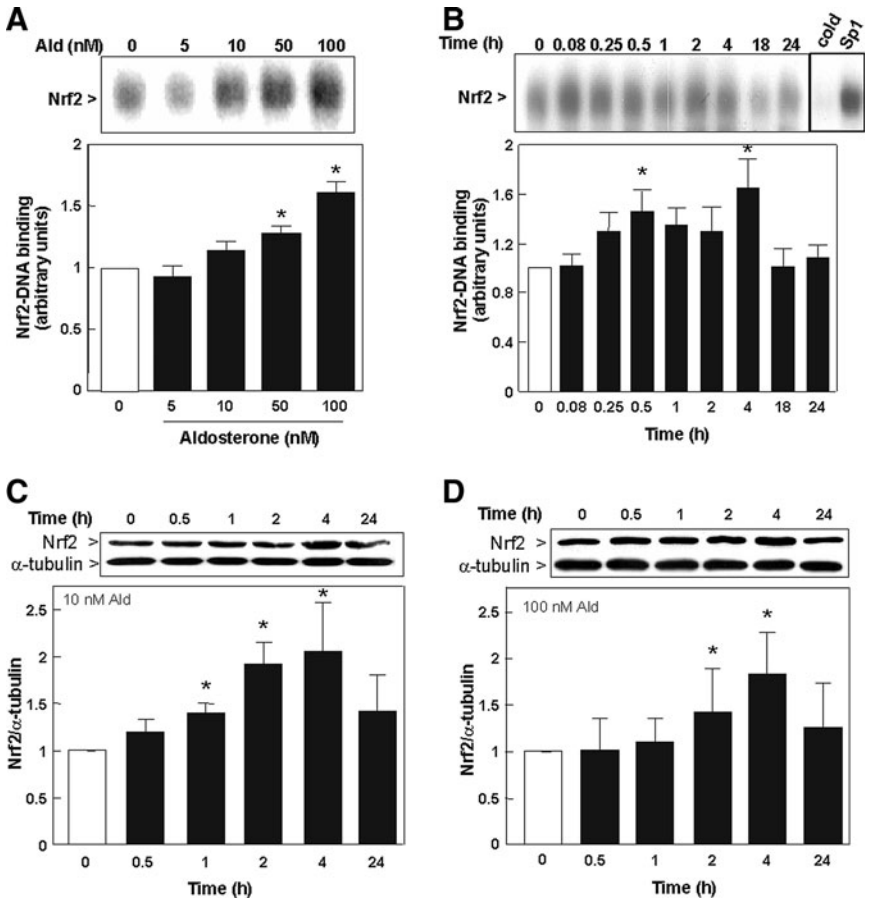

FIG. 2. Aldosterone induces the activation of Nrf2 in LLC-PK1 cells. **(A)** Dose dependency of Nrf2-activation. Nrf2-DNA binding was measured by EMSA in nuclear fractions, incubated in the absence (0) and presence of the indicated aldosterone concentrations for 30 min. **(B)** Kinetics of aldosterone (100 n*M*) induced Nrf2-DNA binding in nuclear fractions as measured by EMSA. To determine the specificity of the Nrf2-DNA complex, the control nuclear fraction (0 h incubation) was incubated in the presence of 100-fold molar excess of unlabeled oligonucleotide containing the consensus sequence for either Nrf2 (cold) or SP-1 (SP-1) before conducting the binding assay. The nuclear presence of Nrf2 (95–110 kDa) was evaluated by Western blot in LLC-PK1 cells that were incubated with **(C)** 10 n*M* aldosterone and **(D)** 100 n*M* aldosterone. α-tubulin was measured as a loading control. Results are shown as ratio of Nrf2/α-tubulin. **(A, B)** Shown are mean values ± SEM, $*p \le 0.05$ *versus* time point 0, tested by ANOVA with subsequent *post-hoc* comparisons by Scheffé. **(C, D)** Shown is the median ± the standard error of the median, $*p \le 0.05$ *versus* time point 0, evaluated by Mann–Whitney test. EMSA, electrophoretic mobility shift assay.

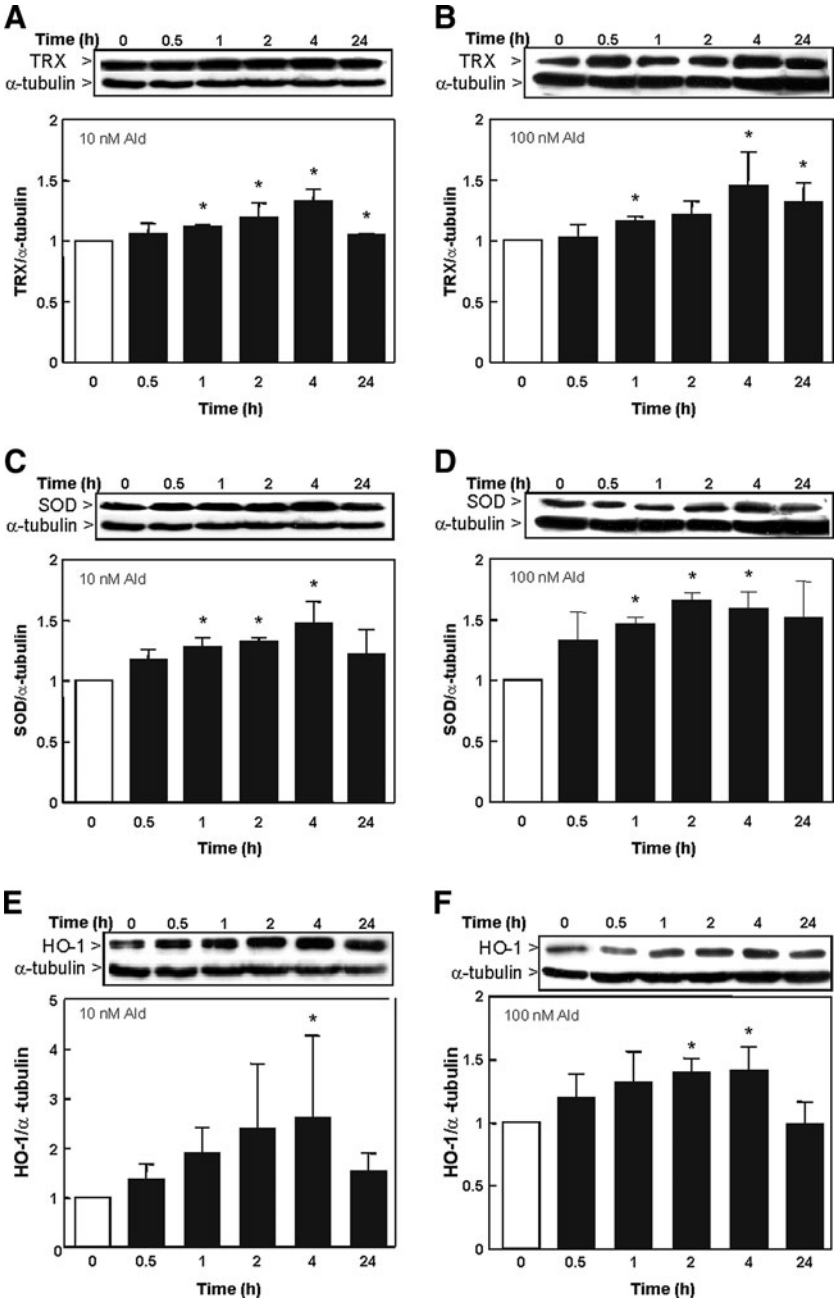

FIG. 3. Expression of Nrf2-regulated proteins in LLC-PK1 cells. The expression of Nrf2-regulated proteins was detected by Western blot in cells incubated in the absence (0) and the presence of 10 **(A, C, E)** and 100 n*M* **(B, D, F)** aldosterone for the indicated time points. Protein levels of **(A, B)** TRX (71 kDa), **(C, D)** SOD (16 kDa), and **(E, F)** HO-1 (32 kDa) were measured and referred to the α-tubulin (50 kDa) content as a loading control. **(A–F)** Shown is the median ± the standard error of the median, $*p \leq 0.05$ *versus* time point 0, evaluated by Mann–Whitney test. SOD, superoxide dismutase; TRX, thioredoxin; HO-1, heme oxygenase-1.

Levels of total glutathione (GSH) were measured by plate reader. After 4 h incubation with 10 n*M* aldosterone, no significant increase in total GSH could be observed (Fig. 4C), which was significant using 100 n*M* aldosterone (Fig. 4D). After 24 h, aldosterone-treated cells showed a trend to lower GSH levels compared to control cells.

Aldosterone-induced activation of Nrf2 is mediated by an increase of reactive oxygen and nitrogen species. To investigate whether aldosterone-triggered Nrf2 activation occurred as a consequence of an increase in cell oxidants, oxidant levels were evaluated using 5-(and-6)-carboxy-2′7′-dichlorodihydro-fluorescein diacetate (H_2DCF-DA), a probe to detect intracellular oxidants (reactive nitrogen species [RNS] and reactive oxygen species [ROS]) (9). Aldosterone triggered a significant increase of DCF fluorescence in LLC-PK1 cells after 15 min incubation, which remained high for approximately 24 h (Fig. 5A, B).

The ratio of reduced to oxidized glutathione (GSH/GSSG) was measured as a parameter of oxidative stress. At both aldosterone concentrations (10 and 100 n*M*), a reduction of the GSH/GSSG ratio was observed after 4 and 24 h incubation compared to controls, underlining a high level of oxidative stress (Fig. 5C, D).

The aldosterone-mediated increase of Nrf2-DNA binding was partially or totally prevented by the simultaneous incubation of cells with the antioxidants N-acetyl cysteine (NAC), (±)-α-lipoic acid (LA), and tempol (Fig. 5E). These findings strongly suggest that aldosterone induces Nrf2 in LLC-PK1 cells mainly through an increase in the cellular production of oxidants.

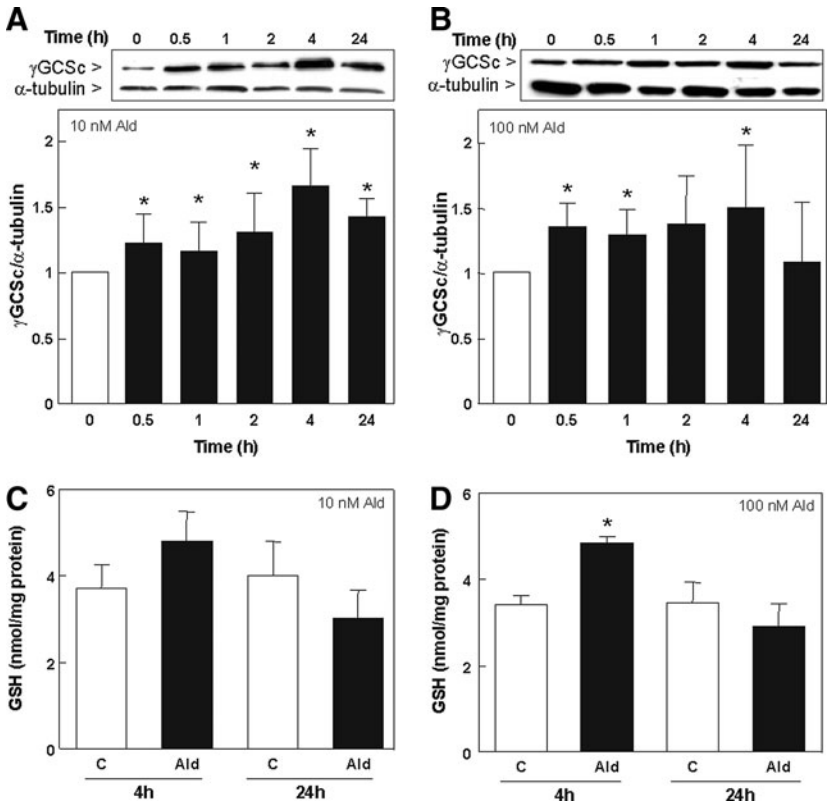

FIG. 4. Effect of aldosterone on GSH synthesis in LLC-PK1 cells. The expression of the Nrf2-regulated protein γGCSc (73 kDa) was detected by Western blot in cells incubated in the absence (0) and the presence of 10 **(A)** and 100 n*M* **(B)** aldosterone for the indicated time points. Protein levels were measured and referred to the α-tubulin (50 kDa) content as loading control. GSH-related fluorescence was measured fluorimetrically at 460 nm (λexc 355 nm) after 4 and 24 h of incubation without (C) or with 10 **(C)** or 100 n*M* **(D)** aldosterone. Results are expressed as fluorescence emission and referred to the protein content. **(A–D)** Shown is the median ± the standard error of the median, $*p \leq 0.05$ *versus* time point 0 or the control group (C), evaluated by Mann–Whitney test.

Aldosterone-induced activation of Nrf2 by oxidants depends on the MR, calcium, protein kinase C, NADPH oxidase, and nitric oxide synthase. LLC-PK1 cells express both the MR and the glucocorticoid receptor (GR) (49), and aldosterone can bind and activate both receptors (46). To investigate whether aldosterone-triggered activation of Nrf2 is mediated exclusively *via* the MR, antagonists of the MR (eplerenone) and the GR (mifepristone) were used. The nuclear Nrf2-binding was significantly reduced after simultaneous incubation with aldosterone and eplerenone, but not with aldosterone and mifepristone. Thus, the activation of Nrf2 in LLC-PK1 cells only required the interaction with the MR (Fig. 6A).

Since aldosterone is known to promote oxidative stress *via* NADPH oxidase, the effects of NADPH oxidase inhibitors on Nrf2 activation were next investigated. LLC-PK1 cells were incubated with aldosterone in the presence of the NADPH oxidase inhibitors diphenyleneiodonium chloride (DPI), apocynin, or 3-benzyl-7-(2-benzoxazolyl)thio-1,2,3-triazolo[4,5-d]pyrimidine) (VAS2870). The three inhibitors significantly reduced aldosterone-induced Nrf2-DNA binding, with VAS2870 being the most potent inhibitor (Fig. 6B).

The involvement of protein kinase C (PKC) in Nrf2 activation was evidenced by the inhibitory action of the PKC inhibitor Ro320432 (Fig. 6B).

To investigate whether aldosterone-induced increased nitric oxide (NO) production contributes to Nrf2 activation, the effects of the NO synthase (NOS) inhibitors L-nitroarginine methyl ester (L-NAME) and N-(6-aminohexyl)-5-chloro-1-naphthalenesulfonamide hydrochloride (W-7) on Nrf2-DNA binding were assessed by EMSA. Both NOS inhibitors prevented aldosterone-mediated Nrf2-DNA binding in LLC-PK1 cells (Fig. 6C).

We recently showed that aldosterone causes an increase in cellular calcium (44), which triggers NADPH oxidase and NOS activation. Accordingly, aldosterone-mediated increase in Nrf2-DNA binding was significantly reduced by the calcium chelator bapta-AM (Fig. 6D).

Activation of Nrf2 is not sufficient to protect the cells against aldosterone-induced oxidative DNA damage. Immunofluorescence staining showed that incubation with 10 and 100 n*M* aldosterone for 4 and 24 h resulted in a significantly increased frequency of DNA double-strand breaks (DSBs), detected as γ-H2AX-foci (Fig. 7A, B and Supplementary Fig. S2A). In addition, the most prominent DNA modification caused by oxidative stress, 7,8-dihydro-8-oxoguanine (8-oxodG), was observed to be significantly increased after 4 h incubation with 10 and 100 n*M* aldosterone, and steadily increased for approximately 24 h (Fig. 7C, D and Supplementary Fig. S2C).

The Nrf2 activator sulforaphane protects cells from aldosterone-induced damage in vitro *and* in vivo

In vitro experiments

Sulforaphane is able to increase the cellular Nrf2 response and protects cells from aldosterone-induced DNA damage. The natural Nrf2 activator sulforaphane was added to aldosterone-treated cells to investigate whether an enhancement of the Nrf2 signal can protect cells against aldosterone-induced DNA damage. Immunofluorescence staining reveals that after 4 h of treatment with 10 and 100 n*M* aldosterone, Nrf2 abundance was significantly increased by aldosterone, but was even more increased by sulforaphane

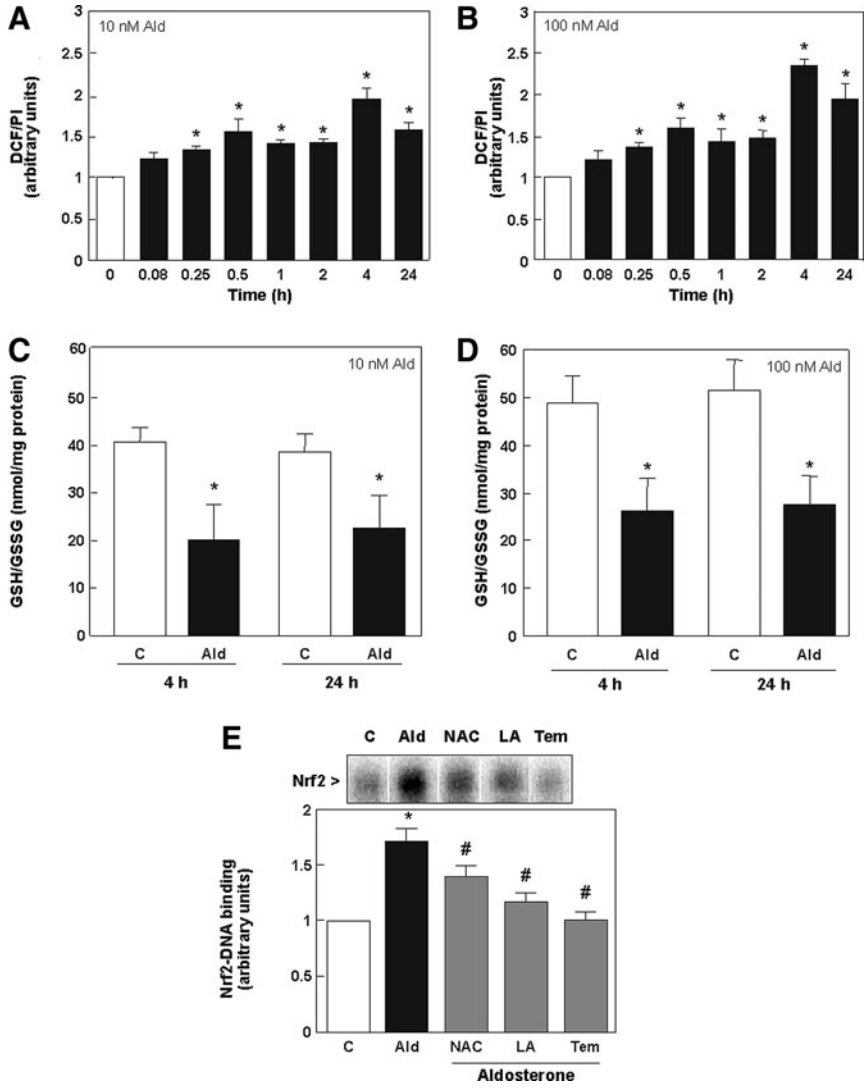

FIG. 5. Aldosterone-induced activation of Nrf2 in LLC-PK1 cells is mediated by an increase of reactive oxygen and nitrogen species. (A) Kinetics of oxidant production caused by aldosterone in LLC-PK1 cells. ROS production was measured using the probe H_2DCF-DA. LLC-PK1 cells were treated for the indicated time periods with 10 or 100 n*M* aldosterone. Oxidation of H_2DCF-DA was detected by monitoring the increase in fluorescence (λexc: 485 nm; λem: 535 nm). **(B)** LLC-PK1 cells were incubated in the absence (C) and presence of 10 and 100 n*M* aldosterone for 4 and 24 h. The GSH/GSSG ratio was measured at 405 nm. Results are expressed as GSH/GSSG ratio. **(C)** LLC-PK1 cells were incubated in the absence (C) and the presence of 100 n*M* aldosterone (Ald) for 30 min. Aldosterone-treated cells were simultaneously incubated with 0.5 m*M* LA (LA), 0.5 m*M* NAC (NAC), or 50 μ*M* tempol (Tem). Nuclear fractions were isolated and analyzed by EMSA. The intensity of the bands corresponding to the Nrf2-DNA complexes was measured. **(A, B, E)** Shown are mean values ± SEM, $^{*}p \le 0.05$ *versus* time point 0, $^{\#}p \le 0.05$ *versus* the aldosterone-treated group, tested by ANOVA with subsequent *post-hoc* comparisons by Scheffé. **(C, D)** Shown is the median ± the standard error of the median, $^{*}p \le 0.05$ *versus* the control group, evaluated by Mann–Whitney test. H_2DCF-DA, 5-(and-6)-carboxy-2′7′-dichlorodihydro-fluorescein diacetate; LA, (±)-α-lipoic acid; NAC, N-acetyl cysteine; Tem, tempol.

alone or by simultaneous treatment with sulforaphane (Fig. 8A, B and Supplementary Fig. S3). Additional treatment with sulforaphane also significantly enhanced the Nrf2 response after 24 h (Fig. 8C). Nevertheless, after 24 h, Nrf2 abundance was altogether lower than after 4 h (Fig. 8D).

Sulforaphane was able to significantly decrease aldosterone-induced DSB detected as γ-H2AX-foci after 4 h (Fig. 9A, B and Supplementary Fig. S4) and 24 h (Fig. 9C). Aldosterone-induced DNA damage was further significantly decreased in the comet assay after 4 h (Fig. 9E) and 24 h (Fig. 9F) treatment with sulforaphane. Representative pictures of the comet assay are shown in Figure 9D and Supplementary Figure S4.

In vivo study

Clinical characteristics and renal function. The potential protective action of the Nrf2 activator sulforaphane was tested in rats treated with aldosterone, sulforaphane/aldosterone, and sulforaphane. No significant changes could be detected in the body weight between the groups (Table 1). The ratio of kidney to body weight was used as an index of renal hypertrophy. The kidney to body weight ratio for both kidneys was significantly increased in the aldosterone group compared to control rats and sulforaphane-treated rats, indicating renal hypertrophy. A significant increase of the urine volume could be detected in the aldosterone group, which was significantly decreased in the sulforaphane/aldosterone group (Table 1). With regard to the creatinine clearance, a slight impairment in the aldosterone-treated group could be observed, whereas a significant increase was revealed in the sulforaphane/aldosterone group compared to the aldosterone-treated group (Table 1). Histopathological parameters of kidney damage (glomerular sclerosis index [GSI] and mesangiolysis index [MSI]) show a clear increase in glomerular and tubular damage in the aldosterone-treated group compared to the control group. Sulforaphane/aldosterone treatment led to a significant decrease in glomerular damage and to a slight decrease in tubular damage (Table 1). Treatment of male Sprague–Dawley rats with aldosterone led to a significant increase of blood pressure compared to control animals. Blood pressure of sulforaphane/aldosterone-treated rats was slightly over the control level, but significantly lower than in the aldosterone-treated group (Table 1). Urinary aldosterone was significantly increased in the aldosterone group compared to

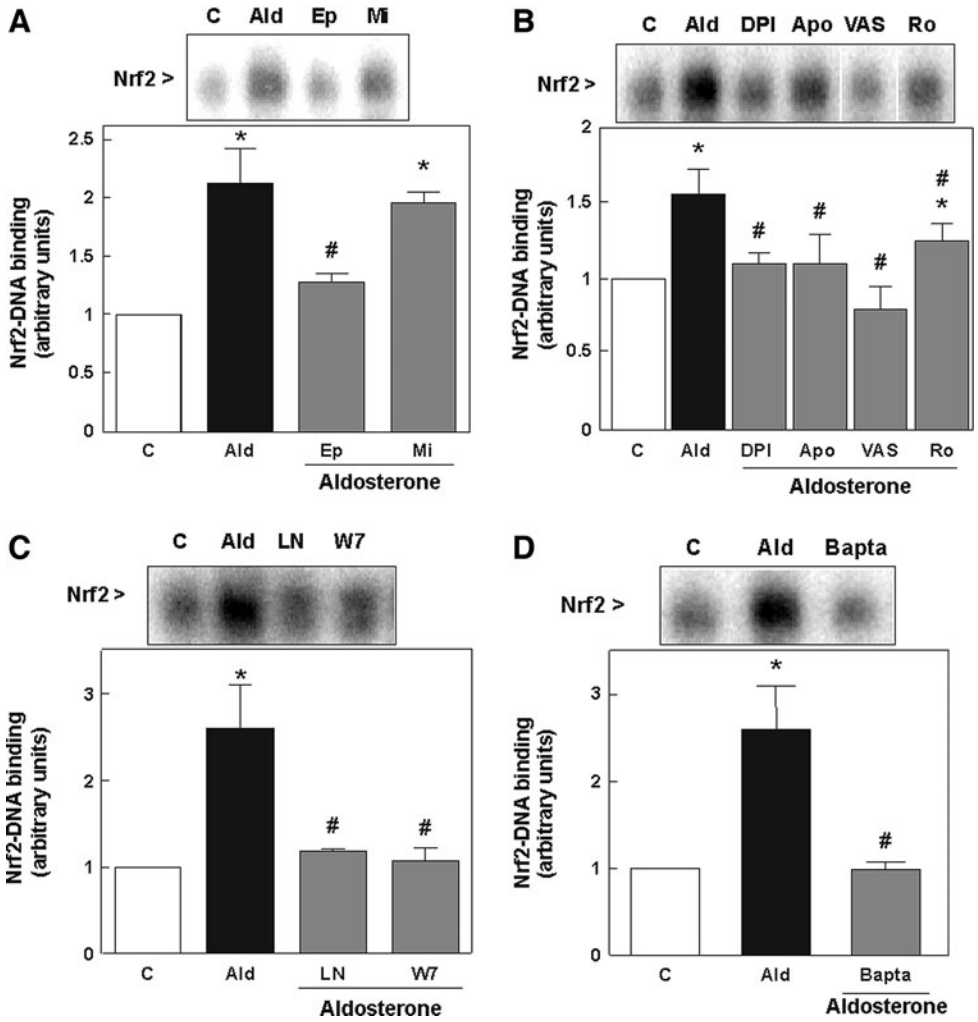

FIG. 6. Aldosterone-induced activation of Nrf2 by oxidants in LLC-PK1 cells depends on the MR, protein kinase C, NADPH oxidase, nitric oxide synthase, and intracellular calcium. (A) The involvement of the MR was evaluated by measuring Nrf2-DNA binding (EMSA) in nuclear fractions from aldosterone-treated cells that were simultaneously incubated without or with either 500 n*M* eplerenone (Ep) or 500 n*M* mifepristone (Mi). LLC-PK1 cells were incubated in the absence (C) and the presence of 100 n*M* aldosterone (Ald) for 4 h. Aldosterone-treated cells were simultaneously incubated with **(B)** 1 μM DPI (DPI), 50 μM apocynin (Apo), 1 μM VAS2870 (VAS) and 1 μM Ro320432 (Ro), **(C)** 50 μM L-NAME (LN), 10 μM W-7 (W7), or **(D)** 10 μM bapta-AM (Bapta). **(A–D)** Shown are mean values ± SEM, $^{*}p \leq 0.05$ *versus* the control group, $^{\#}p \leq 0.05$ *versus* the aldosterone-treated group, tested by ANOVA with subsequent *post-hoc* comparisons by Scheffé. DPI, diphenyleneiodonium chloride; W-7, N-(6-aminohexyl)-5-chloro-1-naphthalenesulfonamide hydrochloride; VAS2870, 3-benzyl-7-(2-benzoxazolyl)thio-1,2,3-triazolo[4,5-d]pyrimidine).

control rats and significantly reduced in the sulforaphane/aldosterone group compared to aldosterone-treated rats. Plasma aldosterone levels were not statistically different between all groups (Table 1). Further, all parameters in sulforaphane-treated rats were not different from control rats.

Sulforaphane is able to increase the Nrf2 response and protects rat kidneys from aldosterone-induced DNA damage. The *in vivo* activation of Nrf2 in rat kidneys was further investigated. As in the first animal experiment, aldosterone-treated rats showed significantly higher levels of Nrf2 in the cortex (Fig. 10A) and in the medulla (Fig. 10B) than control rats. Nrf2 levels were even higher in sulforaphane-treated rat kidneys. The highest Nrf2 abundance in the nuclei could be observed in the sulforaphane/aldosterone group. Representative pictures are shown in Supplementary Figure S5A.

Immunohistochemical staining against the DSB marker γ-H2AX showed a significant increase in DSBs in the cortex (Fig. 10C) and medulla (Fig. 10D) of aldosterone-treated rat kidneys compared to control and sulforaphane-treated rat kidneys. DSBs were significantly reduced in sulforaphane/aldosterone-treated rat kidneys. Representative pictures are shown in Supplementary Figure S5B. Further, in the comet assay, DNA damage was significantly reduced in sulforaphane/aldosterone-treated rats compared to aldosterone-treated rats (Fig. 10E).

Discussion

Nrf2 plays a leading role in the protection against oxidant- and xenobiotic-induced cellular injury. Nrf2 regulates basal activity and the coordinated induction of genes encoding for

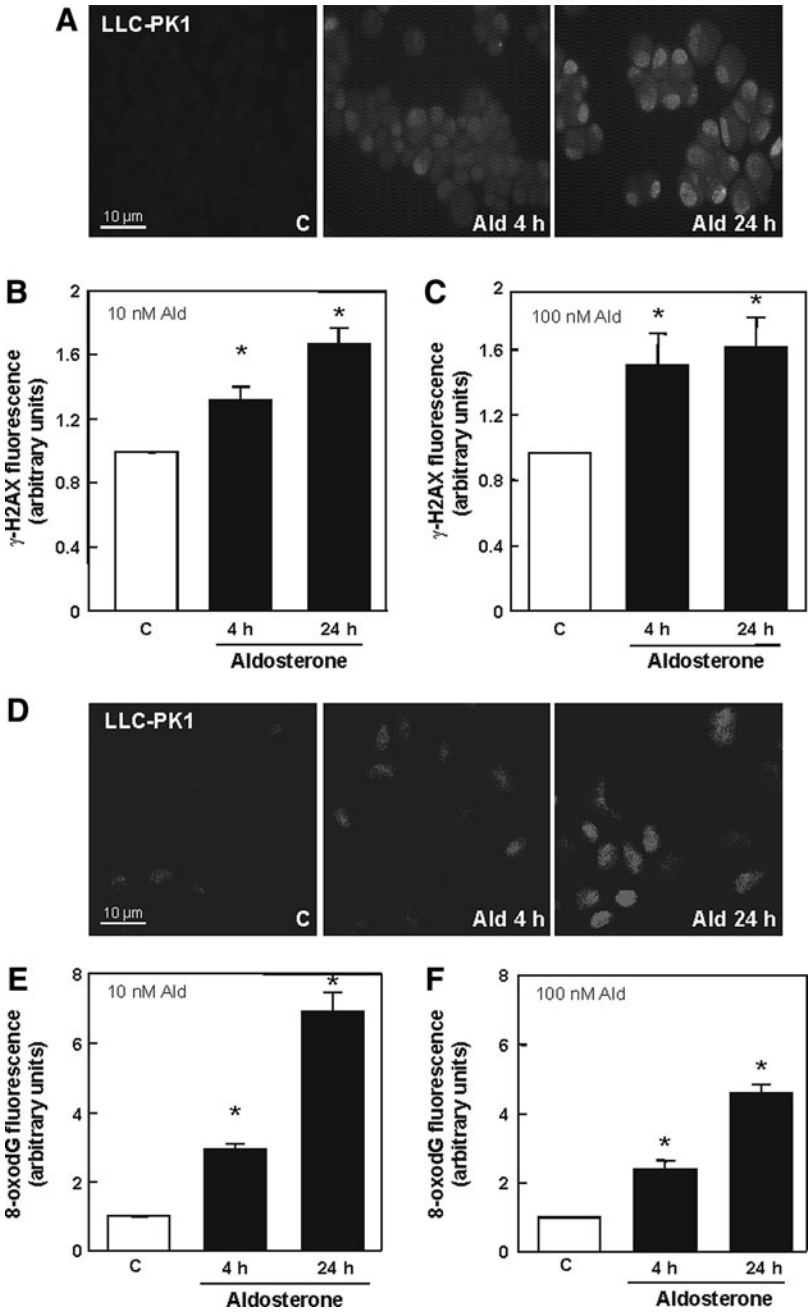

FIG. 7. Aldosterone affects oxidative DNA damage levels in LLC-PK1 cells. (A) Cells were stained for DSBs with an antibody against γ-H2AX. Shown are representative pictures of control cells and cells treated with 100 n*M* aldosterone after the indicated time points. Pictures were taken using a fluorescence microscope: Quantifications were done by measuring gray values of $\sim$150 cells treated with either 10 n*M* **(B)** or 100 n*M* **(C)** aldosterone for the indicated time spans with ImageJ. **(D)** LLC-PK1 cells stained for 8-oxodG lesions. Shown are representative pictures of control cells and cells treated with 10 nM aldosterone after the indicated time points. Pictures were taken by a TCS SP5 laser scanning confocal microscope. Quantifications were done by measuring gray values of $\sim$100 cells treated with either 10 n*M* **(E)** or 100 n*M* **(F)** aldosterone for the indicated time spans with ImageJ. **(B, C, E, F)** Shown is the median $\pm$ the standard error of the median, $*p \leq 0.05$ *versus* the control group, evaluated by Mann–Whitney test. DSBs, double strand breaks. 8-oxodG, 7,8-dihydro-8-oxo-guanine.

proteins involved in the protection against oxidative stress, and phase II detoxifying enzymes. We recently showed in renal cells, as well as in two animal models of mineralocorticoid-induced hypertension, that high levels of aldosterone cause both increased ROS and RNS production, and DNA damage (41–43, 48, 49). This article investigated the potential activation of Nrf2 as a protective response against hyperaldosteronism both *in vitro* and *in vivo*. This is, to the best of our knowledge, the first report showing the activation of Nrf2 by aldosterone. Nrf2 activation by increased aldosterone levels in kidney tubule cells as well as in rat kidneys is dependent on the MR and occurs as a consequence of aldosterone-induced increased production of ROS and/or RNS as indicated by the inhibitory action of MR blockers (eplerenone *in vitro* and spironolactone *in vivo*) and antioxidants such as tempol. Although the activation of Nrf2 initially leads to the induction of oxidant-protective genes such as TRX, SOD, HO-1, and γGCSc and to an increase in GSH levels, long-term aldosterone exposure apparently leads to a decrease in GSH levels and to DNA oxidation and breakage.

NADPH oxidase is one of the major sources of aldosterone-induced ROS production in renal cells (19, 23, 39). In agreement with this, we observed that NADPH oxidase activation leads to aldosterone-mediated Nrf2 activation. This is supported by the finding that NADPH oxidase inhibitors prevented aldosterone-induced Nrf2 activation. In our study, VAS2870 was the most potent NADPH oxidase inhibitor, completely preventing Nrf2 activation. However,

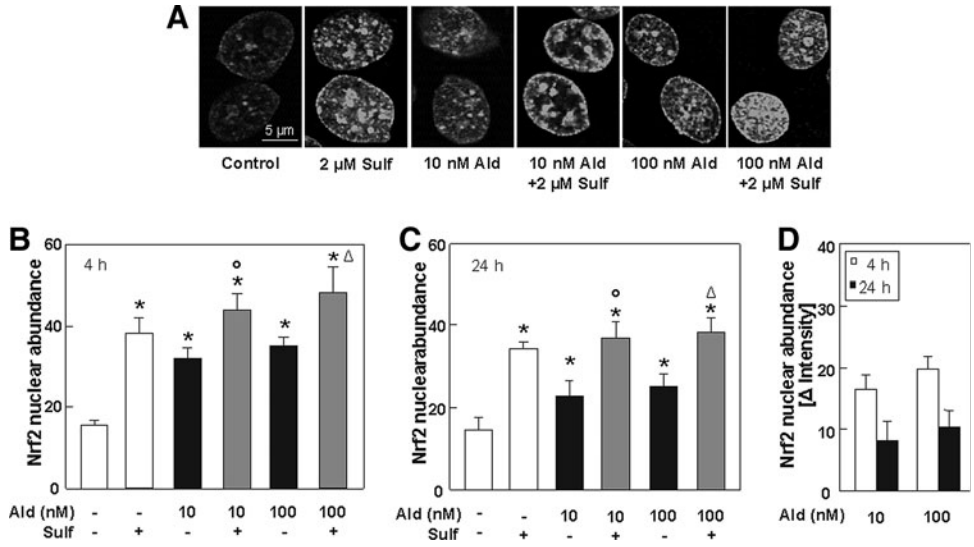

FIG. 8. Sulforaphane increases the cellular Nrf2 response. (A) LLC-PK1 cells were stained for Nrf2-positive nuclei. Shown are representative pictures of control cells and aldosterone- (10 and 100 n*M*) and sulforaphane (2 μM)-treated cells. Pictures were taken by a TCS SP5 laser scanning confocal microscope. Quantifications were done by measuring gray values of $\sim$100 cells per treatment after 4 h **(B)** and 24 h **(C)** with ImageJ. **(D)** Nrf2 nuclear abundance normalized to the respective control after 4 and 24 h of aldosterone treatment. **(B–D)** Shown are mean values $\pm$ SEM, $^{*}p \leq 0.05$ *versus* the control group, $^{\circ}p \leq 0.05$ *versus* 10 n*M* aldosterone alone, $^{\Delta}p \leq 0.05$ *versus* 100 n*M* aldosterone alone, tested by ANOVA with subsequent *post-hoc* comparisons by Scheffé. See Supplementary Figure S3.

NADPH oxidase could act as a double-edged sword. A transient activation can initially provide a feedback antioxidant response through ROS *via* Nrf2. Prolonged NADPH oxidase activation by aldosterone may lead to a depletion of intracellular NADPH, impaired ROS scavenging associated with eNOS uncoupling, mitochondrial dysfunction, and diminished Nrf2-mediated antioxidant gene expression (14).

Since NADPH oxidase can be activated *via* PKC, the PKC inhibitor Ro320432 was used to test the involvement of this enzyme. Aldosterone-induced Nrf2 activation was significantly reduced by the PKC inhibitor Ro320432, suggesting that NADPH oxidase is activated *via* a PKC-dependent pathway. However, PKC can also, independent of NADPH oxidase activation, directly phosphorylate Nrf2, thereby inducing ARE-mediated gene expression (24).

We previously reported that aldosterone activates NOS in LLC-PK1 cells, leading to an increase in NO production (43, 44). We now observed that two NOS inhibitors, L-NAME and W-7, inhibited aldosterone-mediated Nrf2 activation. NOS generates NO, which is known to activate a battery of detoxifying enzymes and other proteins with protective functions (11). Although NOS has generally protective effects on the kidney, excess NO is considered to damage cellular components by reacting with superoxide to generate peroxynitrite (54), which, in turn, is able to activate Nrf2 (27).

Both enzymes, NADPH oxidase and NOS, can be activated by calcium. Aldosterone causes a rapid mobilization of intracellular calcium in different cell types (16, 22, 34). Similarly, we found that aldosterone increases intracellular calcium in LLC-PK1 cells (44). The finding that the calcium chelator bapta-AM prevented aldosterone-induced Nrf2 activation demonstrates the involvement of calcium. The importance of calcium signaling in the activation process of Nrf2 was previously described in human hepatoma cells infected with hepatitis C virus (4).

The coordinated induction of antioxidants and phase II enzymes has been shown to protect cells against toxicity, mutagenicity, and carcinogenicity resulting from the exposure to environmental and synthetic chemicals and drugs (57). Accordingly, we observed that the expression of TRX, SOD, HO-1, and γGCSc increased in aldosterone-treated cells for approximately 4 h, indicating that LLC-PK1 cells initiated a protective Nrf2-dependent response against aldosterone actions. However, the Nrf2 response was not enough to neutralize the adverse effects of a singular aldosterone treatment in LLC-PK1 cells, probably due to the down-regulation of Nrf2-regulated genes after 24 h exposure to aldosterone. *In vivo*, on the other hand, even after 4 weeks of continuous aldosterone treatment, the HO-1 and γGCSc expression was elevated in the Ald group, which in the animal possibly points to a rather chronic induction of Nrf2. These differences between *in vitro* and *in vivo* might result from alterations of cultured cells. Moreover, *in vitro*, only one kidney cell type was studied, while many different cell types are affected by aldosterone *in vivo*. In the light of existing reports, the fact that we see a raised activation of Nrf2 *in vivo* at all is astonishing: In chronic kidney disease, as well as in two hypertension models, the Dahl-sensitive hypertensive rat and the spontaneously hypertensive rat, Nrf2 activity and target gene expression were reduced (6, 28, 60). Only in hypertension induced by the synthetic steroid deoxycorticosterone acetat, an up-regulation was also observed (18).

GSH is the most abundant endogenous antioxidant in eukaryotic cells, and it plays a leading role in the regulation of the redox state. GSH exerts potent antioxidant actions by

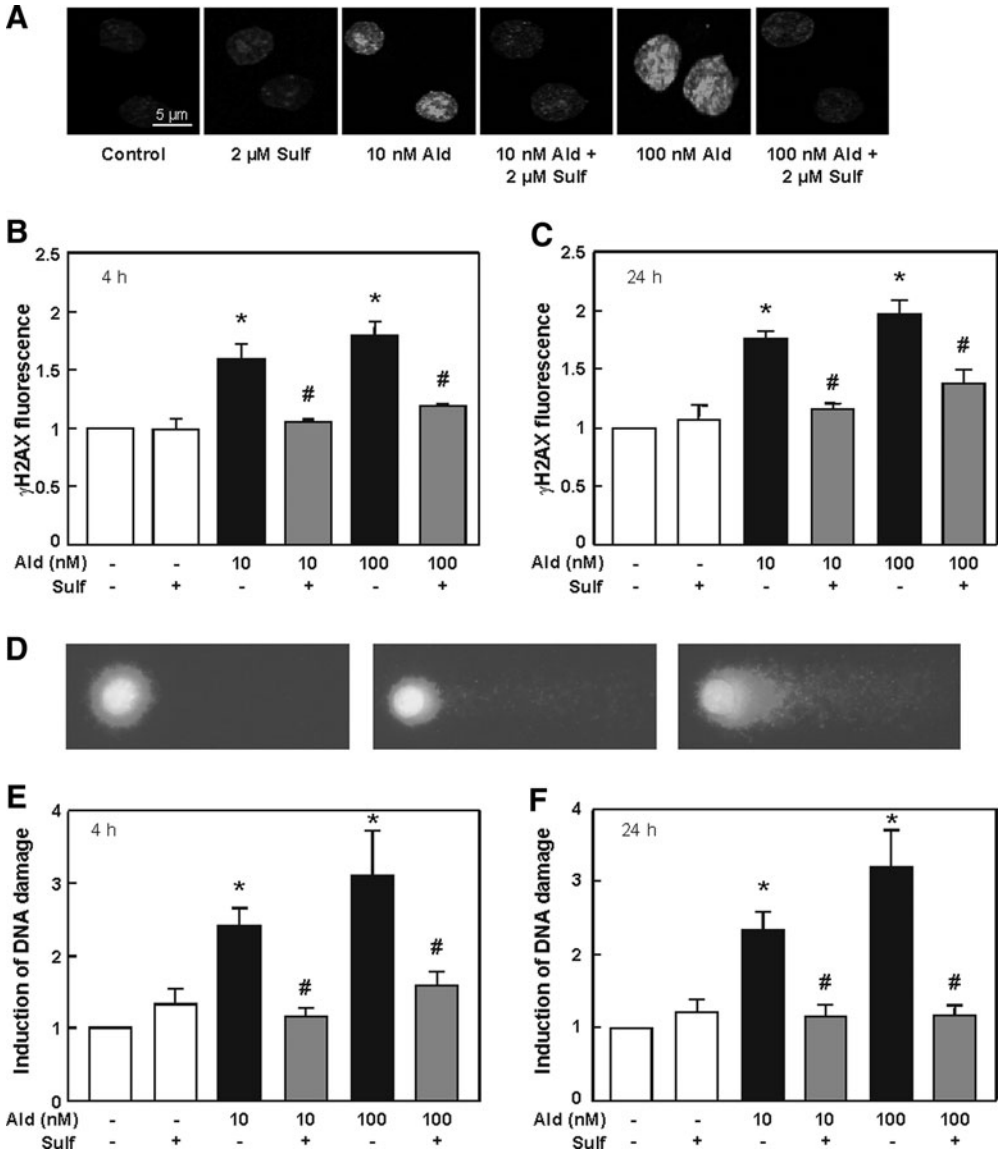

FIG. 9. Sulforaphane protects cells from aldosterone-induced DNA damage. Cells were stained for DSBs with an antibody against γ-H2AX. **(A)** Shown are representative pictures of control cells and aldosterone- (10 and 100 n*M*) and sulforaphane (2 μM)-treated cells for 4 h. Pictures were taken by a TCS SP5 laser scanning confocal microscope. Quantifications were done after 4 h **(B)** and 24 h **(C)** of treatment by measuring gray values of $\sim$150 cells per treatment with ImageJ. **(D)** Representative pictures of nuclei of cells subjected to the comet assay procedure. Left picture: nucleus of an untreated cell, middle and right picture: nuclei of cells treated with aldosterone with different grades of DNA damage. Effects of sulforaphane on aldosterone-induced DNA damage measured by comet assay in LLC-PK1 cells after 4 h **(E)** and 24 h **(F)**. Shown is the induction of DNA damage. (**B, C, E, F**) Shown are mean values $\pm$ SEM, $^{*}p \leq 0.05$ *versus* the control group, $^{\#}p \leq 0.05$ *versus* the respective treatment with aldosterone alone, tested by ANOVA with subsequent *post-hoc* comparisons by Scheffé. See Supplementary Fig. S4.

directly scavenging ROS/RNS and by serving as a substrate in reactions that are catalyzed by a number of major antioxidant enzymes such as GPx. Selective inhibition of the enzymes of the GSH redox cycle heightens the susceptibility to ROS/RNS-mediated cell injury (28). We observed that after 4 h of treatment, aldosterone up-regulated the catalytic subunit of GCL (γGCSc), which resulted in an increase in GSH levels. Increased intracellular GSH levels have been shown to provide greater resistance of cells against acute NO stress (15) and increased oxidative stress (51). Nevertheless, cellular GSH concentrations were decreased again after 24 h of treatment with aldosterone. Consistently, we observed that after 24 h of treatment with aldosterone, ROS levels were still high; while Nrf2 activation returned to basal levels. These findings suggest that Nrf2 activation is a transient process on exposure of LLC-PK1 cells to aldosterone. Although in our animals target genes of Nrf2 were still up-regulated after 4 weeks of treatment with aldosterone, we measured increased markers of oxidative stress in the kidneys of aldosterone-treated rats (41).

Table 1. Body Weight, Kidney/Body Weight Ratio, Urinary and Blood Parameters, Blood Pressure, and Histopathological Parameters in Rats

Parameters	*Control*	*Aldosterone*	*Aldosterone/sulforaphane*	*Sulforaphane*
Body weight (g)	501 ± 11	522 ± 7	516 ± 7	537 ± 7
Kidney/body weight ratio (‰)	3.9 ± 0.2	4.7 ± 0.5*	4.4 ± 0.2	3.8 ± 0.3#
Urine volume (ml)	40 ± 4	83 ± 20*	23 ± 7#	18 ± 3#
Creatinine clearance (ml/min)	94 ± 10	58 ± 5	135 ± 18#	105 ± 6
Glomerular sclerosis index	0.53 ± 0.08	1.05 ± 0.16*	0.54 ± 0.09#	0.46 ± 0.11#
Mesangiolysis index	0.20 ± 0.04	0.44 ± 0.07*	0.32 ± 0.07	0.24 ± 0.05
Blood pressure (mm Hg)	153 ± 5	180 ± 7*	158 ± 2#	147 ± 3#
Aldosterone in plasma (n*M*)	1.4 ± 0.2	1.7 ± .0.2	1.6 ± .0.2	1.4 ± .0.2
Aldosterone in urine (μg/24 h)	0.18 ± 0.03	0.41 ± 0.09*	0.27 ± 0.04#	0.15 ± 0.02#

For body weight, creatinine clearance, blood pressure, and aldosterone in plasma, the mean values ± SEM are shown, *$p \le 0.05$ *versus* the control; #$p \le 0.05$ *versus* the aldosterone-treated group, tested by ANOVA with subsequent *post-hoc* comparisons by Scheffé. For kidney/body weight ratio, urine volume, and aldosterone in urine, the median ± the standard error of the median is shown, *$p \le 0.05$ *versus* the control; #$p \le 0.05$ *versus* the aldosterone-treated group, evaluated by Kruskal–Wallis test with subsequent *post-hoc* comparisons by Dunn.

We found a significant increase of DNA DSBs in aldosterone-treated kidney cells after 4 and 24 h. DSBs are serious lesions that can initiate genomic instability, finally leading to cancer (26, 36). When ROS are sufficiently close to a DNA double-strand helix, multiple lesions can be formed on both strands, leading to DSBs. After DSB formation, large amounts of histone H2AX are phosphorylated to γ-H2AX in the chromatin around the breaking point, thereby creating a focus where proteins involved in DNA repair and chromatin remodeling accumulate. This amplification makes it possible to detect single DSBs with an antibody against γ-H2AX (2). Although Nrf2 activation was maximal at 4 h in aldosterone-treated LLC-PK1 cells, this was not sufficient to protect the cells against the aldosterone-induced increase in cellular ROS/RNS, and, as a consequence, DSBs were still detectable. In addition, aldosterone caused an increase of the oxidized base 8-oxodG. 8-oxodG is one of the most abundant lesions in oxidatively damaged DNA and was found to induce mutations through G-to-T transversions (7). Oxidatively damaged DNA has been recognized to be associated with the

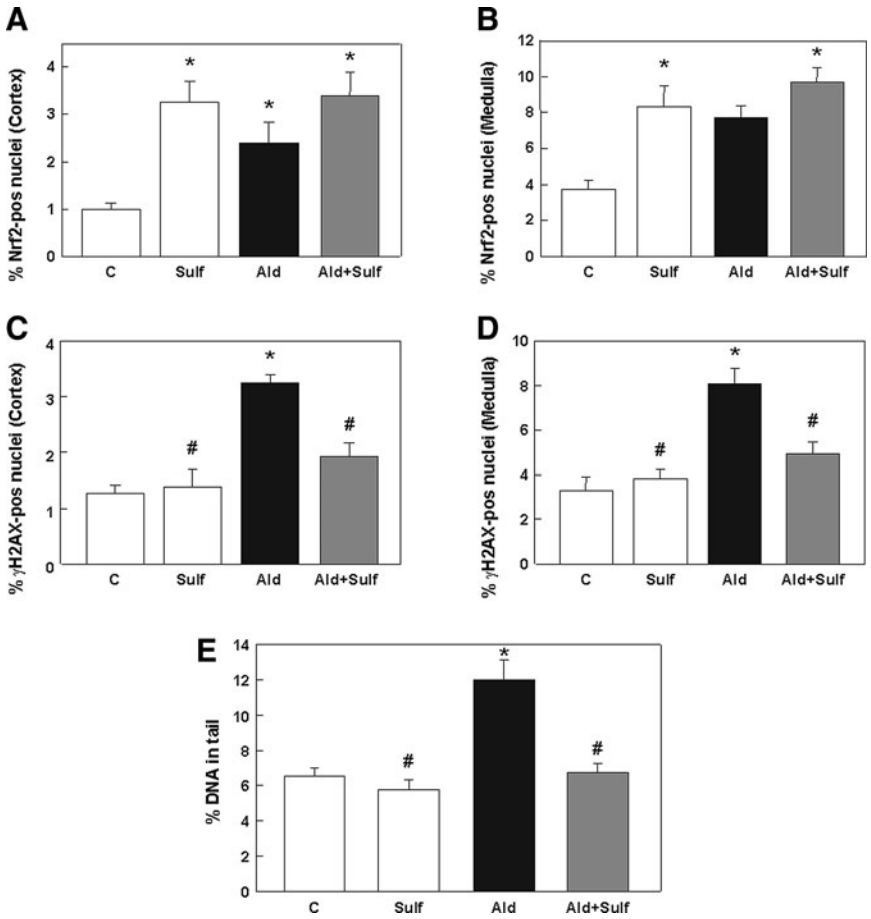

FIG. 10. Sulforaphane increases the Nrf2 response and protects rat kidneys from aldosterone-induced DNA damage. Evaluation of immunohistochemical staining on paraffin-embedded kidney cortex and medulla sections for Nrf2 activation. The ratio of positive/negative nuclei was quantified by Cell Profiler within eight visual fields of cortex **(A)** and medulla **(B)** of the kidney. Evaluation of immunohistochemical staining on paraffin-embedded kidney cortex and medulla sections for γ-H2AX activation. The ratio of positive/negative nuclei was quantified by Cell Profiler within eight visual fields of the cortex **(C)** and medulla **(D)** of the kidney. **(E)** DNA damage measured by the comet assay in kidney cells extracted from kidneys of all groups. Results are shown as percentage of DNA in the tail. **(A–E)** Shown are mean values ± SEM, *$p \le 0.05$ *versus* the control group, #$p \le 0.05$ *versus* the aldosterone-treated group, tested by ANOVA with subsequent *post-hoc* comparisons by Scheffé.

development of some degenerative diseases, essential hypertension (37), and cancer, including kidney tumors (8, 21). Nrf2 is able to protect cells from oxidative DNA damage *in vivo*: Nrf2-deficient, but not wild-type, mice that are exposed to diesel exhaust particles showed increased levels of 8-oxodG in bronchial epithelial cells (1, 38), pointing out the importance of Nrf2 in the fight against oxidative DNA damage. Although Nrf2 activation was observed in our animal study, a high amount of DNA damage was found in aldosterone-treated rat kidneys (41), indicating that the response was not strong enough to protect the animals against these effects.

To clarify whether known Nrf2 activators could enhance the Nrf2 response to protect cells against aldosterone-induced DNA damage, the isothiocyanate sulforaphane, abundant in cruciferous vegetables such as broccoli or Brussels sprouts, was tested in our study. Sulforaphane was, indeed, able to intensify the Nrf2 response in cells treated with aldosterone after 4 and 24 h. Importantly, sulforaphane was also able to prevent aldosterone-induced DSB, detected as γ-H2AX-foci after 4 and 24 h, and further aldosterone-induced DNA damage after 4 and 24 h in the comet assay.

In vivo, aldosterone treatment induced systemic arterial hypertension, kidney hypertrophy, and impaired kidney function. Sulforaphane/aldosterone treatment improved most of these effects: Urine volume was lowered compared to aldosterone-treated rats, and creatinine clearance was significantly higher than in aldosterone-treated rats. In addition, histopathological parameters such as glomerular and tubular damage were, in part, significantly decreased in this group. As observed in our first animal experiment (41), blood pressure was significantly increased after aldosterone treatment compared to control rats. In comparison to the aldosterone-treated group, sulforaphane/aldosterone treatment significantly reduced blood pressure down to control levels. In aldosterone-treated animals, the plasma aldosterone concentration was about 2 n*M*, corresponding to the plasma level of patients suffering from resistant hypertension (47). Since plasma aldosterone levels were not statistically different between all groups, this hints at a possible systemic internal regulation of aldosterone plasma levels. Urinary aldosterone was significantly increased in the aldosterone group compared to control rats and significantly reduced in the sulforaphane and sulforaphane/aldosterone group compared to aldosterone-treated rats. One explanation could be that in aldosterone-treated rats, the renin-angiotensin-aldosterone system is up-regulated, which seems to be somehow prevented by sulforaphane.

The improvement of arterial hypertension and kidney function by sulforaphane treatment could be due to an additional increase of Nrf2 in the kidney cortex and medulla compared with aldosterone-treated rats. Recently, the Nrf2-activating substance bardoxolone methyl, a synthetic triterpenoid, was tested in a phase 3 study due to its potentially nephroprotective effects (10, 40). The clinical study had to be stopped due to serious adverse effects (10). Additional knowledge on Nrf2 actions in the kidney and on the effects of Nrf2 activators of other substance classes than triterpenoids might give new perspectives for further trials. Sulforaphane treatment also led to a significant reduction of DNA damage in the comet assay and DSBs (γ-H2AX-foci) compared to aldosterone-treated rats. DNA damage has long been recognized as an important factor in aging and cellular senescence (53), but lately, it has also been considered a contributor to disease progression due to the generation of dysfunctional cells (25). Furthermore, the DNA damage response was recently connected to progressive loss-of-kidney function (31). Therefore, the results pointing out the beneficial effects of sulforaphane in aldosterone-treated rats could be the starting point for further studies aiming at therapies against end-organ damage in hypertension or kidney cancer.

The present work shows that *in vitro*, aldosterone initially triggered the activation of Nrf2 as a protective antioxidant response in LLC-PK1 cells. Although antioxidant or detoxifying enzymes, such as TRX, SOD, HO-1, or γGCSc, were rapidly induced in response to aldosterone-induced oxidative or nitrative stress, this adaptive survival response seemed to be transient and overwhelmed by a chronic increased production of ROS/RNS. As a consequence, oxidative DNA damage occurred. Further, although Nrf2 activation was observed *in vivo*, a high amount of DNA damage was found in aldosterone-treated rat kidneys, indicating that the response was not strong enough to protect the animals against these effects, which could, in part, underlie the higher cancer mortality observed in hypertensive patients, who often present elevated aldosterone levels. Therapies enhancing the Nrf2 response could prevent the adverse effects of aldosterone on the kidney, heart, and aorta and, therefore, the possible oncogenic action in hypertensive patients.

Materials and Methods

Materials

Epithelial porcine kidney cells with proximal tubular properties (LLC-PK1) were obtained from the American Type Culture Collection. Cell culture medium and reagents were obtained from PAA Laboratories GmbH. The primary antibodies against γGCSc (sc-22755) and Nrf2 (sc-722) were obtained from Santa Cruz Biotechnology. HO-1 (2212-1) was purchased from Epitomics, 8-oxoG (SQP003.1) was obtained from Squarix, γ-H2AX (AP07419PU-N) was obtained from Acris Antibodies GmbH, SOD1 (GTX100554) and TrxR1 (GTX108727) antibodies were purchased from Biozol, α-tubulin (T6199) was obtained from Sigma, and gapdh (2118S) was purchased from Cell Signaling Technology, Inc. The secondary antibody Cy3-conjugated AffiniPure F(ab')$_2$ fragment goat anti-rabbit IgG (111-166-045) was purchased from Jackson Immunoresearch and CF™488A (20015) from Biotium. The oligonucleotides containing the consensus sequence for Nrf2 and SP-1 and the reagents for the EMSA were obtained from Promega. Polyvinylidene fluoride (PVDF) membranes were obtained from Bio-Rad, and Chroma Spin-10 columns were obtained from Clontech. The ECL plus Western blotting system was from Amersham Pharmacia Biotech, Inc. H_2DCF-DA and propidium iodide (PI) were obtained from Molecular Probes. Apocynin was obtained from Calbiochem. Aldosterone, 1,2-bis(2-aminophenoxy) ethane-N,N,N′,N′-tetraacetic acid tetrakis(acetoxymethyl) ester (BAPTA-AM), DPI, eplerenone, L-NAME, W-7, mifepristone (Mi), Ro320432 (Ro), L-sulforaphane (Sulf), tempol, and all other reagents were obtained from the highest quality available and were purchased in Sigma. D,L-Sulforaphane (Sulf) was obtained from Santa Cruz Biotechnology. VAS2870 was kindly donated by Vasopharm BIOTECH GmbH.

Methods

Cell culture. LLC-PK1 cells were cultured for 24 h in control medium, as described earlier (49). Cells were, subsequently, treated with aldosterone (5–100 n*M*) for 0.08–24 h, depending on the assay. Previous evidence showed that concentrations of aldosterone of approximately 100 n*M* and 24 h incubation do not affect LLC-PK1 cell viability (43).

Animal treatment

First animal experiment. Thirty-two male Sprague–Dawley (RjHan:SD) rats (Janvier) were randomly divided into four groups at the age of 5–6 weeks (8 per group). After 3 weeks of acclimatization, group 2–4 received 0.75 μg/h.kg aldosterone for 4 weeks *via* an osmotic minipump (Alzet, 2 ml) to induce a mineralocorticoid-dependent hypertension. Group 1 (Control) received PBS *via* an osmotic minipump. In addition, all animals got 1% (w/v) NaCl in the drinking water. Compared with group 2 (Ald), group 3 (spironolactone/Ald) was given daily 25 mg/kg spironolactone per gavage in addition to aldosterone and group 4 (tempol/Ald) 1 m*M* tempol *via* the drinking water.

Second animal experiment. Twenty-nine male Sprague–Dawley (RjHan:SD) rats (Janvier) were randomly divided into four groups at the age of 5–6 weeks (eight per group, exception: five in the sulforaphane group). After 3 weeks of acclimatization, group 3–4 (Ald and sulforaphane/Ald) received 0.75 μg/h.kg aldosterone for 4 weeks *via* an osmotic minipump (Alzet, 2 ml) to induce a mineralocorticoid-dependent hypertension. Group 1 (Control) and 2 (sulforaphane) received PBS *via* the osmotic minipump. In addition, all animals got 1% (w/v) NaCl in the drinking water. Group 4 (sulforaphane/Ald) and group 2 (sulforaphane) were given 15 mg/kg D,L-sulforaphane *via* drinking water. Blood pressure was measured once a week noninvasively by the tail-cuff method (Visitech Systems). At the beginning and at the end of the experiment, the rats were placed in metabolic cages, and urine samples were collected after 24 h for assessing renal function.

After 4 weeks of treatment, the animals of both experiments were anesthesized (ketamine 120 mg/kg and xylazine 8 mg/kg i.m.), the organs of the animals were perfused with ice-cold 0.9% (w/v) NaCl solution (Fresenius Kabi) and Deltadex 40 (AlleMan Pharma) containing 1% (w/v) procain hydrochloride, and the kidneys were excised. All animal experiments were performed in accordance with the European Community guidelines for the use of experimental animals and with the German law for the protection of animals. The investigation conforms to the Guide for the Care and Use of Laboratory Animals published by the US National Institutes of Health (NIH Publication No. 85-23, revised 1996).

Electrophoretic mobility shift assay. Nuclear fractions were isolated as previously described (35). For the EMSA, the oligonucleotides containing the consensus sequence of Nrf2 or SP-1 were end labeled with [γ-^{32}P]-ATP using T4 polynucleotide kinase and purified using Chroma Spin-10 columns. Samples were incubated with the labeled oligonucleotide (20,000–30,000 cpm) for 20 min at room temperature in 1 × binding buffer (5 × binding buffer: 50 m*M* Tris-HCl buffer, pH 7.5, containing 20% [v/v] glycerol, 5 m*M* $MgCl_2$, 2.5 m*M* EDTA, 2.5 m*M* dithiothreitol (DTT), 250 m*M* NaCl, and 0.25 mg/ml poly[dI-dC]). The products were separated by electrophoresis in a 6% (w/v) nondenaturing polyacrylamide gel using 0.5 × TBE (Tris/borate 45 m*M*, EDTA 1 m*M*) as the running buffer. The gels were dried, and the radioactivity was quantified in a Phosphorimager 840 (Amersham Pharmacia Biotech, Inc.).

Evaluation of the concentration of intracellular oxidants. The concentration of intracellular oxidants was estimated using the probe H_2DCF-DA. Cells were seeded in 96-well plates and at confluency, they were incubated in medium with or without 10 or 100 n*M* aldosterone for 0.08–24 h. During the last 5 min of treatment, cells were additionally loaded with 40 μM H_2DCF-DA. Fluorescence was measured at λexc: 485 nm; λem: 535 nm. Afterwards, cells were rinsed with PBS, and 200 μl of PBS was added per well. To determine DNA content, samples were incubated with 0.1% (v/v) Igepal for 20 min and, subsequently, with 50 μM PI, incubated for 30 min at room temperature, and the fluorescence (λexc: 544 nm, λem: 568 nm) was measured. Results are expressed as ratio of DCF fluorescence/PI fluorescence.

Western blot analysis. For the preparation of total cell extracts, 5×10^6 cells were rinsed with PBS, scraped, and centrifuged. The pellet was rinsed with PBS, and resuspended in 200 μl of 50 m*M* HEPES (pH 7.4), 125 m*M* KCl, which contained protease inhibitors and 1% (v/v) Igepal. The final concentration of the inhibitors was 0.5 m*M* PMSF, 1 mg/L leupeptin, 1 mg/L pepstatin, 1.5 mg/L aprotinin, 2 mg/L bestatin, and 0.4 m*M* sodium pervanadate. Samples were exposed to one cycle of freezing and thawing, incubated at 4°C for 30 min, and centrifuged at 15,000 *g* for 30 min. The supernatant was decanted, and the protein concentration was measured (3). Nuclear fractions were isolated as previously described (35).

For the preparation of kidney extracts, one quarter of each rat kidney was minced on nitrogen, suspended in lysis buffer (50 m*M* Tris, 150 m*M* NaCl, 1 m*M* EDTA, 0.25% sodium desoxycholate, and 1% Nonidet p40), and finally centrifuged at 8000 *g* at 4°C for 5 min. The supernatant was transferred to a new tube, and protein concentration was measured (3).

Approximately 40–50 μg protein were separated by reducing 10% (w/v) or 12.5% (w/v) SDS-PAGE and electroblotted to PVDF membranes. Membranes were blocked for 2 h in 5% (w/v) bovine serum albumin; incubated in the presence of corresponding primary antibodies Nrf2 (1:500), γGclc (1:1000), and HO-1 (1:1000) overnight, β-tubulin (1:1000) for 90 min at 37°C, and gapdh (1:2000) for 60 min at room temperature. After incubation for 90 min at room temperature in the presence of the secondary antibody (horseradish peroxidase [HRP]-conjugated) (1:10,000 dilution), the conjugates were visualized by chemiluminescence detection in a Phosphorimager 840 (Amersham Pharmacia Biotech, Inc.).

GSH/GSSG determination. LLC-PK1 cells (0.2×10^5) seeded the previous day were treated with test substances for 4 and 24 h. Cells were washed with ice-cold 1 × PBS, centrifuged at 1000 *g* for 5 min at 4°C, and incubated with extraction buffer (0.1% Triton X-100, 0.6% sulfosalicylic acid, and 0.1 *M* potassium phosphate EDTA buffer). Cells

were homogenized by ice-cold sonication in an ultrasonic bath for 2–3 min, and centrifuged at 3000 *g* for 4 min at 4°C. The supernatant was separated for GSH (200 μl) and GSSG (100 μl) determination into different tubes. In addition, GSH (1 mg/ml) and GSSG (2 mg/ml) standard curves were prepared. GSH samples were kept on ice, and 2 μl of 1 *M* 2-vinylpyridine was added to GSSG samples/standards and incubated for 1 h at room temperature. Afterwards, 6 μl of 1.14 *M* triethanolamine was added to GSSG samples/standards and incubated for 10 min at room temperature. All samples were kept on ice until measurements were taken. Standards and samples were added to a 96-well plate; 0.2 U GSH reductase, 60 μl of 1.68 m*M* 5,5′-dithio-bis(2-nitrobenzoic acid), and 60 μl of 0.8 m*M* NADPH were loaded; and finally, absorption was measured at 405 nm by plate reader. Protein content was determined by Bradford (29). Results are expressed as the ratio of GSH/GSSG absorption/protein content.

Fluorimetric determination of GSH levels. LLC-PK1 cells (0.18×10^5) seeded the previous day were treated with test substances for 4 and 24 h. Cells were washed with ice-cold 1 × PBS and incubated with 1 ml of lysis buffer (0.2 *M* mannitol, 50 m*M* saccharose, 0.01 *M* HEPES, and pH 7.5) for 10 min on ice. Afterwards, the cells were scraped, transferred into a tube, and centrifuged at 12,000 *g* for 10 min at 4°C. Cell lysates were collected into a new microcentrifuge tube, and 90 μl of the samples were added to a 96-well plate (Fluotrac 200, black; Greiner Bio-One GmbH). Ten microliters of 17.65 m*M* monochlorobimane (4 mg/ml PBS) was loaded to all wells and incubated for 1–2 h in the dark at room temperature. Fluorescence was recorded using a fluorescence plate reader with a 355/460 nm filter set. Protein content was determined by Bradford (29). Results are expressed as the ratio of GSH fluorescence/protein content.

Detection of phosphorylated γ-H2AX sites. LLC-PK1 cells seeded the previous day were treated with test substances for 4 and 24 h, harvested, brought onto glass slides by cytospin centrifugation, and fixed in ice-cold methanol for 24 h. The coverslips were washed twice with PBS; incubated overnight at 37°C with anti-γ-H2AX antibody (AP07419PU-N; Acris Antibodies GmbH); and, after extensive washing with PBS containing 0.2% Tween (PBST), they were incubated for 30 min at 37°C in the dark with a fluorescein isothiocyanate-conjugated secondary antibody. Nuclei were counterstained with Hoechst 33258, and the slides were mounted with DABCO (1,4-diazabicyclo(2.2.2)octan). Images were captured using a Nikon Eclipse 55i fluorescence microscope (Nikon GmbH) at a 400-fold magnification. Quantification was done by measuring gray values of 100 cells per treatment with ImageJ 1.40g (http://rsb.info.nih.gov/ij/) (45).

Detection of 8-oxodG by immunofluorecent staining. LLC-PK1 cells seeded the previous day were treated with test substances for 4 and 24 h. Cells were harvested, brought onto glass slides by cytospin centrifugation, and fixed in ice-cold methanol for 24 h. RNA was digested with 200 μg/ml RNAse A, 50 U/ml RNAse T1 for 1 h at 37°C. After incubating the cells in 60% 70 m*M* NaOH, 140 m*M* NaCl, and 40% methanol for 5 min at 0°C, the cells were proteolyzed in 0.1% trypsin for 30 s at 37°C. Proteinase K (2 μg/ml in 20 m*M* Tris/HCl and 2 m*M* $CaCl_2$, pH 7.5) was added for 10 min at 37°C, and the cells were washed in PBS and 0.2% glycin/PBS. Blocking was performed in 1% casein/PBS for 30 min at room temperature followed by overnight incubation with anti-8-oxoG antibody (SQP003.1; Squarix) at 4°C. The next day, cells were washed in 0.05% Tween/PBS, and a Cy3-labeled secondary antibody (1:700) was added for 1 h at room temperature. After washing, the cells were stained with 4′,6-diamidin-2-phenylindol (DAPI) and mounted with confocal matrix. Confocal images were obtained by measuring the fluorescence at 570 nm (λexc 550 nm) and 660 nm (λexc 633 nm) using a sequential scan with a TCS SP5 laser scanning confocal microscope (Leica Microsystems GmbH). Quantification was done by measuring gray values of 100 cells per treatment with ImageJ 1.40g (http://rsb.info.nih.gov/ij/) (45).

Nuclear abundance of Nrf2 observed by confocal microscopy. LLC-PK1 cells (0.3×10^5) were seeded in 6-well plates on cover slips and treated with test substances for 4 and 24 h. Cells were washed and fixed in ice-cold methanol for 7 min. After blocking for 1 h in blocking solution (10% fetal calf serum, 1% Tween 20), cells were incubated with the primary Nrf2 antibody (1:100) for 2 h at room temperature, washed, and, subsequently, incubated with the CF™488A-labeled secondary antibody (1:500) for 1 h at room temperature in the dark. Cells were stained with DAPI and mounted with confocal matrix. Confocal images were obtained by measuring the fluorescence at 515 nm (λexc 488 nm) with a TCS SP5 laser scanning confocal microscope (Leica Microsystems GmbH). Quantification was done by measuring gray values of 100 cells per treatment with ImageJ 1.40g (http://rsb.info.nih.gov/ij/) (45).

Extraction of primary kidney cells. Freshly obtained rat kidney parts were minced on ice to small pieces, which were suspended in 3 ml buffer consisting of RPMI 1640, 15% DMSO, and 1.8% (w/v) NaCl. The extracted primary rat kidney cells were sifted through a cell strainer with a mesh pore size of 100 μM (Becton Dickinson), centrifuged for 5 min at 1000 rpm and at 4°C, and, finally, resuspended in 1 ml of buffer. Cells were kept on ice until the comet assay was performed.

Comet assay. The comet assay was done as described earlier (50). Briefly, cells were treated for 4 and 24 h with the tested substances. Afterwards, the cells were embedded in agarose and exposed to an electrical field. From cells with damaged DNA (single-strand breaks or DSBs, alkali labile sites), more DNA can migrate than from cells with intact nuclear DNA. A comet-like structure is formed, because smaller fragments and relaxed loops move faster than larger fragments and intact DNA. DNA was stained with PI (20 μg/ml). A fluorescence microscope at 200-fold magnification and a computer-aided image analysis system (Komet 5; Kinetic Imaging Ltd.) were used for analysis. Fifty cells in total (25 per slide) were analyzed per experimental condition performed at least in triplicate, and the results were expressed as percentage of DNA in the tail region.

Immunohistochemistry. Immunohistochemistry was performed by using a commercially available tyramide signal amplification kit (Perkin Elmer) according to the protocol provided by the manufacturer. Briefly, paraffin kidney sections (2 μM) were mounted on glass slides, heated at 60°C for 1 h, and deparaffinized. The sections were incubated with 3% (v/v) hydrogen peroxide for 20 min at room temperature, washed, and boiled in citrate buffer (10 m*M* citric acid, 2 *M* NaOH) for 1 h. Afterward, the slides were blocked with TNB buffer for 30 min at room temperature, incubated with 0.001% (w/v) avidin and 0.001% (w/v) biotin, subsequently with the primary anti-Nrf2 antibody (1:1000 dilution) overnight at 4°C, followed by a 1 h incubation with the biotin-conjugated secondary antibody (1:100 dilution). Sections were incubated with streptavidin-HRP (1:100) for 30 min, followed by tyramide amplification (10 min) and another streptavidin-HRP incubation for 30 min. Slides were incubated with diaminobenzidine chromogen (Vector Laboratories) for 8 min, counterstained with hematoxylin, and mounted with Eukitt (Fluka). Pictures were taken with a Leica DM 750 microscope at 200-fold magnification, using a Leica ICC50 HD camera. The ratio of positive/negative nuclei was assessed using the cell image analysis software CellProfiler (30) within eight visual fields.

Assessment of urinary and blood parameters. Creatinine in urine and serum was analyzed by a commercially available ELISA kit (Cayman Chemicals) according to the protocol provided by the manufacturer. Briefly, a standard curve was prepared, samples were analyzed in duplicates, and, finally, the absorbance was measured at 490 nm in a plate reader. Creatinine clearance was calculated from urinary and serum values. Aldosterone was measured in urine and plasma using a commercially available ELISA kit (Biotrend) according to the manufacturer's protocol. Urine samples were diluted in urine diluent (Biotrend).

Histopathology. For histopathological investigation of the kidney, 2 μM sections were cut and stained with periodic acid-Schiff stain. In the kidneys, GSI and MSI were determined as described earlier (59).

Statistical analysis. All animal data and multiple comparisons were analyzed by one-way analysis of variance (ANOVA), and subsequent *post-hoc* comparisons by Scheffé were performed using Statview 5.0.1 (Brainpower, Inc.) or SPSS 21 (IBM), after ensuring normal distribution with the Shapiro–Wilk test. Values are given as mean ± SEM. Of experiments with less than six independent repetitions, non-normal distribution was assumed and these and other non-normal distributed data were analyzed with the Mann–Whitney test or by the Kruskal–Wallis test with subsequent comparisons by Dunn. Here, the median and the standard error of the median are shown. A p-value ≤ 0.05 was considered statistically significant. All experiments were performed at least thrice.

Acknowledgments

The authors thank Kathrin Happ, Laura Vogel, and Sabine Gärtner for excellent technical assistance. This work was supported by grants from the University of California, Davis, USA (to P.I.O.), the Deutsche Forschungsgemeinschaft, Germany, Grant Schu 2367/1-2 (to N.S. and H.S.) and Grant Schu 2367/5-1 (to N.S.), and by a research fellowship from the University of Würzburg, Germany (to N.Q.).

Author Disclosure Statement

No competing financial interests exist.

References

1. Aoki Y, Sato H, Nishimura N, Takahashi S, Itoh K, and Yamamoto M. Accelerated DNA adduct formation in the lung of the Nrf2 knockout mouse exposed to diesel exhaust. *Toxicol Appl Pharmacol* 173: 154–160, 2001.
2. Bonner WM, Redon CE, Dickey JS, Nakamura AJ, Sedelnikova OA, Solier S, and Pommier Y. GammaH2AX and cancer. *Nat Rev Cancer* 8: 957–967, 2008.
3. Bradford MM. A rapid and sensitive method for the quantitation of microgram quantities of protein utilizing the principle of protein-dye binding. *Anal Biochem* 72: 248–254, 1976.
4. Burdette D, Olivarez M, and Waris G. Activation of transcription factor Nrf2 by hepatitis C virus induces the cell-survival pathway. *J Gen Virol* 91: 681–690, 2010.
5. Calhoun DA, Jones D, Textor S, Goff DC, Murphy TP, Toto RD, White A, Cushman WC, White W, Sica D, *et al.* Resistant hypertension: diagnosis, evaluation, and treatment: a scientific statement from the American Heart Association Professional Education Committee of the Council for High Blood Pressure Research. *Circulation* 117: e510–e526, 2008.
6. Chen TM, Li J, Liu L, Fan L, Li XY, Wang YT, Abraham NG, and Cao J. Effects of heme oxygenase-1 upregulation on blood pressure and cardiac function in an animal model of hypertensive myocardial infarction. *Int J Mol Sci* 14: 2684–2706, 2013.
7. Cheng KC, Cahill DS, Kasai H, Nishimura S, and Loeb LA. 8-Hydroxyguanine, an abundant form of oxidative DNA damage, causes G—T and A—C substitutions. *J Biol Chem* 267: 166–172, 1992.
8. Cooke MS, Olinski R, and Evans MD. Does measurement of oxidative damage to DNA have clinical significance? *Clin Chim Acta* 365: 30–49, 2006.
9. Crow JP. Dichlorodihydrofluorescein and dihydrorhodamine 123 are sensitive indicators of peroxynitrite *in vitro*: implications for intracellular measurement of reactive nitrogen and oxygen species. *Nitric Oxide* 1: 145–157, 1997.
10. de Zeeuw D, Akizawa T, Agarwal R, Audhya P, Bakris GL, Chin M, Krauth M, Lambers Heerspink HJ, Meyer CJ, McMurray JJ, *et al.* Rationale and trial design of bardoxolone methyl evaluation in patients with chronic kidney disease and type 2 diabetes: the occurrence of renal events (BEACON). *Am J Nephrol* 37: 212–222, 2013.
11. Dhakshinamoorthy S and Porter AG. Nitric oxide-induced transcriptional up-regulation of protective genes by Nrf2 via the antioxidant response element counteracts apoptosis of neuroblastoma cells. *J Biol Chem* 279: 20096–20107, 2004.
12. Friis S, Sorensen HT, Mellemkjaer L, McLaughlin JK, Nielsen GL, Blot WJ, and Olsen JH. Angiotensin-converting enzyme inhibitors and the risk of cancer: a population-based cohort study in Denmark. *Cancer* 92: 2462–2470, 2001.

13. Funder J and New MI. Low renin hypertension (LRH): shades of John Laragh. *Trends Endocrinol Metab* 19: 83, 2008.
14. Gao L and Mann GE. Vascular NAD(P)H oxidase activation in diabetes: a double-edged sword in redox signalling. *Cardiovasc Res* 82: 9–20, 2009.
15. Gegg ME, Beltran B, Salas-Pino S, Bolanos JP, Clark JB, Moncada S, and Heales SJ. Differential effect of nitric oxide on glutathione metabolism and mitochondrial function in astrocytes and neurones: implications for neuroprotection/neurodegeneration? *J Neurochem* 86: 228–237, 2003.
16. Gekle M, Freudinger R, Mildenberger S, and Silbernagl S. Aldosterone interaction with epidermal growth factor receptor signaling in MDCK cells. *Am J Physiol Renal Physiol* 282: F669–F679, 2002.
17. Gius D and Spitz DR. Redox signaling in cancer biology. *Antioxid Redox Signal* 8: 1249–1252, 2006.
18. Gomez-Guzman M, Jimenez R, Sanchez M, Zarzuelo MJ, Galindo P, Quintela AM, Lopez-Sepulveda R, Romero M, Tamargo J, Vargas F, *et al.* Epicatechin lowers blood pressure, restores endothelial function, and decreases oxidative stress and endothelin-1 and NADPH oxidase activity in DOCA-salt hypertension. *Free Radic Biol Med* 52: 70–79, 2012.
19. Griendling KK, Sorescu D, and Ushio-Fukai M. NAD(P)H oxidase: role in cardiovascular biology and disease. *Circ Res* 86: 494–501, 2000.
20. Grossman E, Messerli FH, Boyko V, and Goldbourt U. Is there an association between hypertension and cancer mortality? *Am J Med* 112: 479–486, 2002.
21. Habib SL, Danial E, Nath S, Schneider J, Jenkinson CP, Duggirala R, Abboud HE, and Thameem F. Genetic polymorphisms in OGG1 and their association with angiomyolipoma, a benign kidney tumor in patients with tuberous sclerosis. *Cancer Biol Ther* 7: 23–27, 2008.
22. Harvey BJ and Higgins M. Nongenomic effects of aldosterone on Ca2+ in M-1 cortical collecting duct cells. *Kidney Int* 57: 1395–1403, 2000.
23. Hayashi H, Kobara M, Abe M, Tanaka N, Gouda E, Toba H, Yamada H, Tatsumi T, Nakata T, and Matsubara H. Aldosterone nongenomically produces NADPH oxidase-dependent reactive oxygen species and induces myocyte apoptosis. *Hypertens Res* 31: 363–375, 2008.
24. Huang HC, Nguyen T, and Pickett CB. Regulation of the antioxidant response element by protein kinase C-mediated phosphorylation of NF-E2-related factor 2. *Proc Natl Acad Sci U S A* 97: 12475–12480, 2000.
25. Jackson SP and Bartek J. The DNA-damage response in human biology and disease. *Nature* 461: 1071–1078, 2009.
26. Jeggo PA and Lobrich M. DNA double-strand breaks: their cellular and clinical impact? *Oncogene* 26: 7717–7719, 2007.
27. Kang KW, Choi SH, and Kim SG. Peroxynitrite activates NF-E2-related factor 2/antioxidant response element through the pathway of phosphatidylinositol 3-kinase: the role of nitric oxide synthase in rat glutathione S-transferase A2 induction. *Nitric Oxide* 7: 244–253, 2002.
28. Kim HJ and Vaziri ND. Contribution of impaired Nrf2-Keap1 pathway to oxidative stress and inflammation in chronic renal failure. *Am J Physiol Renal Physiol* 298: F662–F671, 2010.
29. Kruger NJ. The Bradford method for protein quantitation. *Methods Mol Biol* 32: 9–15, 1994.
30. Lamprecht MR, Sabatini DM, and Carpenter AE. CellProfiler: free, versatile software for automated biological image analysis. *Biotechniques* 42: 71–75, 2007.
31. Lans H and Hoeijmakers JH. Genome stability, progressive kidney failure and aging. *Nat Genet* 44: 836–838, 2012.
32. Lau A, Villeneuve NF, Sun Z, Wong PK, and Zhang DD. Dual roles of Nrf2 in cancer. *Pharmacol Res* 58: 262–270, 2008.
33. Leckie C, Chapman KE, Edwards CR, and Seckl JR. LLC-PK1 cells model 11 beta-hydroxysteroid dehydrogenase type 2 regulation of glucocorticoid access to renal mineralocorticoid receptors. *Endocrinology* 136: 5561–5569, 1995.
34. Losel RM, Feuring M, Falkenstein E, and Wehling M. Nongenomic effects of aldosterone: cellular aspects and clinical implications. *Steroids* 67: 493–498, 2002.
35. Mackenzie GG, Zago MP, Keen CL, and Oteiza PI. Low intracellular zinc impairs the translocation of activated NF-kappa B to the nuclei in human neuroblastoma IMR-32 cells. *J Biol Chem* 277: 34610–34617, 2002.
36. McKinnon PJ and Caldecott KW. DNA strand break repair and human genetic disease. *Annu Rev Genomics Hum Genet* 8: 37–55, 2007.
37. Naganuma T, Nakayama T, Sato N, Fu Z, Soma M, Yamaguchi M, Shimodaira M, Aoi N, and Usami R. Haplotype-based case-control study on human apurinic/apyrimidinic endonuclease 1/redox effector factor-1 gene and essential hypertension. *Am J Hypertens* 23: 186–191, 2010.
38. Osburn WO and Kensler TW. Nrf2 signaling: an adaptive response pathway for protection against environmental toxic insults. *Mutat Res* 659: 31–39, 2008.
39. Paravicini TM and Touyz RM. NADPH oxidases, reactive oxygen species, and hypertension: clinical implications and therapeutic possibilities. *Diabetes Care* 31 Suppl 2: S170–S180, 2008.
40. Pergola PE, Raskin P, Toto RD, Meyer CJ, Huff JW, Grossman EB, Krauth M, Ruiz S, Audhya P, Christ-Schmidt H, *et al.* Bardoxolone methyl and kidney function in CKD with type 2 diabetes. *N Engl J Med* 365: 327–336, 2011.
41. Queisser N, Amann K, Hey V, Habib SL, and Schupp N. Blood pressure has only minor influence on aldosterone-induced oxidative stress and DNA damage *in vivo. Free Radic Biol Med* 54: 17–25, 2013.
42. Queisser N, Fazeli G, and Schupp N. Superoxide anion and hydrogen peroxide-induced signaling and damage in angiotensin II and aldosterone action. *Biol Chem* 391: 1265–1279, 2010.
43. Queisser N, Oteiza PI, Stopper H, Oli RG, and Schupp N. Aldosterone induces oxidative stress, oxidative DNA damage and NF-kappaB-activation in kidney tubule cells. *Mol Carcinog* 50: 123–135, 2011.
44. Queisser N, Schupp N, Stopper H, Schinzel R, and Oteiza PI. Aldosterone increases kidney tubule cell oxidants through calcium-mediated activation of NADPH oxidase and nitric oxide synthase. *Free Radic Biol Med* 51: 1996–2006, 2011.
45. Rasband WS. Image J Software Program. U.S. National Institute of Health, Bethesda, MD, 1997–2008.
46. Rogerson FM, Yao YZ, Elsass RE, Dimopoulos N, Smith BJ, and Fuller PJ. A critical region in the mineralocorticoid receptor for aldosterone binding and activation by cortisol: evidence for a common mechanism governing ligand

binding specificity in steroid hormone receptors. *Mol Endocrinol* 21: 817–828, 2007.
47. Rossi GP, Bernini G, Caliumi C, Desideri G, Fabris B, Ferri C, Ganzaroli C, Giacchetti G, Letizia C, Maccario M, *et al.* A prospective study of the prevalence of primary aldosteronism in 1,125 hypertensive patients. *J Am Coll Cardiol* 48: 2293–2300, 2006.
48. Schupp N, Kolkhof P, Queisser N, Gartner S, Schmid U, Kretschmer A, Hartmann E, Oli RG, Schafer S, and Stopper H. Mineralocorticoid receptor-mediated DNA damage in kidneys of DOCA-salt hypertensive rats. *FASEB J* 25: 968–978, 2011.
49. Schupp N, Queisser N, Wolf M, Kolkhof P, Barfacker L, Schafer S, Heidland A, and Stopper H. Aldosterone causes DNA strand breaks and chromosomal damage in renal cells, which are prevented by mineralocorticoid receptor antagonists. *Horm Metab Res* 42: 458–465, 2010.
50. Schupp N, Schmid U, Rutkowski P, Lakner U, Kanase N, Heidland A, and Stopper H. Angiotensin II-induced genomic damage in renal cells can be prevented by angiotensin II type 1 receptor blockage or radical scavenging. *Am J Physiol Renal Physiol* 292: F1427–F1434, 2007.
51. Shih AY, Johnson DA, Wong G, Kraft AD, Jiang L, Erb H, Johnson JA, and Murphy TH. Coordinate regulation of glutathione biosynthesis and release by Nrf2-expressing glia potently protects neurons from oxidative stress. *J Neurosci* 23: 3394–3406, 2003.
52. Skott O, Uhrenholt TR, Schjerning J, Hansen PB, Rasmussen LE, and Jensen BL. Rapid actions of aldosterone in vascular health and disease—friend or foe? *Pharmacol Ther* 111: 495–507, 2006.
53. Stenvinkel P and Larsson TE. Chronic kidney disease: a clinical model of premature aging. *Am J Kidney Dis* 62: 339–351, 2013.
54. Surh YJ, Kundu JK, Li MH, Na HK, and Cha YN. Role of Nrf2-mediated heme oxygenase-1 upregulation in adaptive survival response to nitrosative stress. *Arch Pharm Res* 32: 1163–1176, 2009.
55. Surh YJ, Kundu JK, and Na HK. Nrf2 as a master redox switch in turning on the cellular signaling involved in the induction of cytoprotective genes by some chemopreventive phytochemicals. *Planta Med* 74: 1526–1539, 2008.
56. Surh YJ and Na HK. NF-kappaB and Nrf2 as prime molecular targets for chemoprevention and cytoprotection with anti-inflammatory and antioxidant phytochemicals. *Genes Nutr* 2: 313–317, 2008.
57. Talalay P, Fahey JW, Holtzclaw WD, Prestera T, and Zhang Y. Chemoprotection against cancer by phase 2 enzyme induction. *Toxicol Lett* 82: 173–179, 1995.
58. Weber KT. Aldosterone in congestive heart failure. *N Engl J Med* 345: 1689–1697, 2001.
59. Westhoff JH, Hilgers KF, Steinbach MP, Hartner A, Klanke B, Amann K, and Melk A. Hypertension induces somatic cellular senescence in rats and humans by induction of cell cycle inhibitor p16INK4a. *Hypertension* 52: 123–129, 2008.
60. Yisireyili M, Shimizu H, Saito S, Enomoto A, Nishijima F, and Niwa T. Indoxyl sulfate promotes cardiac fibrosis with enhanced oxidative stress in hypertensive rats. *Life Sci* 92: 1180–1185, 2013.

Address correspondence to:
Dr. Nina Queisser
Institute of Pharmacology and Toxicology
Versbacher Str. 9
97078 Würzburg
Germany

E-mail: queisser@toxi.uni-wuerzburg.de

Date of first submission to ARS Central, July 31, 2013; date of final revised submission, February 3, 2014; date of acceptance, February 8, 2014.

Abbreviations Used

γGCSc = γ-glutamylcysteine synthetase catalytic subunit
8-oxodG = 7,8-dihydro-8-oxo-guanine
ARE = antioxidant response element
BAPTA-AM = 1,2-bis(2-aminophenoxy)ethane-N,N,N′,N′-tetraacetic acid tetrakis(acetoxymethyl) ester
DABCO = 1,4-diazabicyclo(2.2.2)octan
DAPI = 4′,6-diamidin-2-phenylindol
DCF = 5-(and-6)-carboxy-2',7'-dichlorofluorescein
DPI = diphenyleneiodonium chloride
DSBs = double-strand breaks
DTT = dithiothreitol
EMSA = electrophoretic mobility shift assay
GCL = glutamate cysteine ligase
GPx = glutathione peroxidase
GR = glucocorticoid receptor
GSH = glutathione
GSI = glomerular sclerosis index
H_2DCF-DA = 5-(and-6)-carboxy-2′7′-dichlorodihydro-fluorescein diacetate
HO-1 = heme oxygenase-1
HRP = horseradish peroxidase
Keap1 = Kelch-like ECH-associated protein 1
LA = (±)-α-lipoic acid
L-NAME = L-nitroarginine methyl ester
MR = mineralocorticoid receptor
MSI = mesangiolysis index
NAC = N-acetyl cysteine
NO = nitric oxide
NOS = NO synthase
Nrf2 = nuclear factor-erythroid-2-related factor 2
PI = propidium iodide
PKC = protein kinase C
PVDF = polyvinylidene fluoride
RNS = reactive nitrogen species
Ro = Ro320432
ROS = reactive oxygen species
SOD = superoxide dismutase
TRX = thioredoxin
VAS2870 = 3-benzyl-7-(2-benzoxazolyl)thio-1,2,3-triazolo[4,5-d]pyrimidine)
W-7 = N-(6-aminohexyl)-5-chloro-1-naphthalenesulfonamide hydrochloride